

ELECTRODYNAMICS OF MAGNETARS III: PAIR CREATION PROCESSES IN AN ULTRA-STRONG MAGNETIC FIELD AND PARTICLE HEATING IN A DYNAMIC MAGNETOSPHERE

CHRISTOPHER THOMPSON
CITA, 60 St. George St., Toronto, ON M5S 3H8, Canada
Submitted to the Astrophysical Journal

ABSTRACT

We consider the details of the QED processes that create electron-positron pairs in magnetic fields approaching and exceeding 10^{14} G. The formation of free and bound pairs is addressed, and the importance of positronium dissociation by thermal X-rays is noted. We calculate the collision cross section between an X-ray and a gamma ray, and point out a resonance in the cross section when the gamma ray is close to the threshold for pair conversion. We also discuss how the pair creation rate in the open-field circuit and the outer magnetosphere can be strongly enhanced by instabilities near the light cylinder. When the current has a strong fluctuating component, a cascade develops. We examine the details of particle heating, and show that a high rate of pair creation can be sustained close to the star, but only if the spin period is shorter than several seconds. The dissipation rate in this turbulent state can easily accommodate the observed radio output of the transient radio-emitting magnetars, and even their infrared emission. Finally, we outline how a very high rate of pair creation on the open magnetic field lines can help to stabilize a static twist in the closed magnetosphere and to regulate the loss of magnetic helicity by reconnection at the light cylinder.

Subject headings: plasmas — radiation mechanisms: non-thermal — stars: magnetic fields, neutron

1. INTRODUCTION

Even when not emitting bright bursts of X-rays, magnetars continue to show dramatic variability on much longer timescales. Much of this variability appears to be a consequence of a dynamic magnetosphere. Various manifestations include extremely bright and persistent hard X-ray emission, which can outstrip the loss of rotational energy by a thousand times (Kuiper et al. 2004, 2006); extreme changes in spindown torque that grow and decay over a period of months and can, in some cases, be sustained for years (Kaspi et al. 2001; Woods et al. 2002, 2007; Camilo et al. 2007a, Camilo et al. 2008); and, recently, the discovery of high-frequency radio pulsations from two magnetars (Camilo et al. 2006; 2007b). A general review of magnetars can be found in Woods & Thompson (2006).

This long-term variability appears to be connected only indirectly to the sudden, disruptive events known as Soft Gamma Repeater (SGR) bursts. Increases in spindown torque in the SGRs and some Anomalous X-ray Pulsars (AXPs) typically follow the X-ray bursts by a period of months. Very large torque variations are possible even if the transient X-ray output of the star is quite modest, as in the radio magnetar XTE J1810–197 (Camilo et al. 2007a). Even more remarkably, given the presence of strong torque variability, is the strong clustering of the spin periods of most magnetars within the range of 5–12 seconds. The decay of an internal magnetic field, which ultimately powers the magnetospheric activity, should not be sensitive to the details of current flow and pair creation in the magnetosphere.

Basic energetic considerations suggest that most of the dissipation responsible for the very bright, hard X-ray emission of magnetars is probably concentrated in the closed magnetosphere (Thompson & Beloborodov 2005; Baring & Harding 2007). The inner magnetosphere of a magnetar can sustain much stronger electric currents than the open-field circuit. Thompson, Lyutikov, & Kulkarni (2002) pointed out that starquakes create magnetospheric twists that store an enormous amount of energy in the toroidal magnetic field, enough to supply the observed non-thermal output for a period of years. Beloborodov & Thompson (2007) showed that the voltage in the inner magnetosphere is regulated by a continual e^{\pm} discharge. The electric field that accelerates the particles in the magnetosphere is sustained by the self-induction of the circuit, and the loss of energy by radiation induces a gradual decay in the twist.

It has also been suggested that relatively strong currents flow within the outer magnetosphere of a magnetar, being sustained by the outward transfer of magnetic helicity from an inner zone where it is injected. The redistribution of the twist into the outer magnetosphere causes the poloidal field lines to expand slightly, thereby increasing the open-field voltage (Thompson et al. 2002). This effect depends on the extraction of a tiny fraction of the helicity that is stored in the inner magnetosphere, and therefore does not require a large net input of toroidal field energy into the magnetosphere.

Considerations of the stability of a twisted magnetosphere, and observations of strong variations in the brightness of the radio magnetars on short timescales (Camilo et al. 2007a, 2008), suggest that the twist in the outer magnetosphere is strongly dynamic. A first investigation of pair creation in a dynamic magnetosphere was given by Lyutikov & Thompson (2005), with application to the radio eclipses of the double pulsar system J0737–3039. They noted that strong heating of the particles in the outer magnetosphere would result from a cascade to high spatial frequencies.

In this paper we consider the formation of electron-positron discharges in the case where the outer magnetosphere is strongly dynamic. As a first step, we return to first principles and reconsider the basic mechanisms of pair creation in some detail. Previous theoretical work on e^{\pm} creation and radio death line for magnetars was inconclusive. Baring & Harding (1998, 2001) suggested

that high-energy photons cannot create pairs because they split in the ultrastrong field. This suppression of pair creation would, however, take place only if both polarization modes are able to split, a selection rule which is not supported by microphysical calculations of this process (Adler 1971; Usov 2002). In particular, resonantly scattered photons convert very quickly to e^\pm when $B > 4B_Q$.

Magnetars are bright sources of thermal (keV) X-rays, and gamma rays are created at a high rate close to the star through resonant scattering of the X-rays. The scattered gamma rays propagating through the curved magnetic field can be expected to convert adiabatically to bound electron-positron pairs (Herold, Ruder, & Wunner 1985; Shabad & Usov 1986). We review this process and identify some peculiar features in super-QED magnetic fields. The dissociation of bound pairs depends on the presence of a source of ionizing photons (Usov & Melrose 1996; Potekhin & Pavlov 1997). In addition to photoionization by infrared photons, we identify the resonant scattering of thermal X-rays by one of the bound charges as an effective dissociation channel.

We also reconsider the creation of pairs by collisions between gamma rays and thermal X-rays. The cross section for this process has been calculated previously using wave functions for the magnetized electrons and positrons that are not good eigenstates of the spin (Kozlenkov & Mitrofanov 1986). We recalculate the cross section, finding a slightly different result when the two colliding photons are both below the threshold for single-photon pair creation. We also identify a near resonance in the collision cross section when one of the photons is close to the pair creation threshold.

The period clustering of magnetars might, at first sight, appear to mark out the location of a radio death line in the $P-\dot{P}$ plane. The combined results of this paper, and a companion paper (Thompson 2008), suggest the existence of at least two distinct regimes of pair creation: a more active regime in which the outer magnetosphere is a dynamic reservoir of magnetic helicity and the pair density is extremely high; and a more quiescent regime in which pair creation occurs at more modest rate, and the radio emission is concentrated closer to the star. In this paper, the mechanism of particle heating in the dynamic state is considered self-consistently, along with the energy and multiplicity of the heated pairs. Pair creation occurs mainly via resonant scattering of thermal X-rays close to the surface of the star. A critical spin period arises from the requirement that the heated charges can emit enough pair-creating gamma rays to compensate their loss from the circuit.

Many features of the radio magnetars – their strong flux variability, hard radio spectra, and broad pulses – connect them with the more dynamic circuit behavior described here. The voltage that can be achieved on the more quiescent circuit is examined in detail in Thompson (2008), where it is shown that the power dissipated can barely explain the observed output of the radio magnetars, but is quite sufficient for more standard pulsar emission. The spin clustering of magnetars then signifies a limiting spin period for the more dynamic and intense regime of pair creation. Pulsed radio emission in the more quiescent regime should be possible at significantly longer spin periods (e.g. Medin & Lai 2007).

The plan of the paper is as follows. We consider the conversion of resonantly scattered photons to pairs in §2, and collisions between gamma rays and thermal X-rays in §3. The formation of pairs on a magnetic flux rope with a dynamic twist is treated in §4. An explanation is given in §5.2 for which current driven instabilities in the outer magnetosphere could be regulated by a high rate of pair creation on the open magnetic field lines. Possible sources of short-timescale variations in the open-field voltage are examined in §5. It is shown in §6 that most of the accumulated spindown of a magnetar can occur when its magnetosphere is in the active state. The paper closes with a summary of our results in §7. The Appendix provides details of the calculation of the matrix elements for $\gamma + \gamma \rightarrow e^+ + e^-$ in an ultrastrong magnetic field.

2. CREATION OF PAIRS VIA RESONANT SCATTERING OF THERMAL X-RAYS

The voltage on the open magnetic field lines of a neutron star (and in the closed magnetosphere if it is non-potential) is regulated by pair creation. We focus in this section and §3 on the creation of pairs by energetic gamma rays. The background magnetic field will generally be assumed to be comparable to, or stronger than, the QED field

$$B_Q = \frac{m_e c^3}{e \hbar} = 4.4 \times 10^{13} \text{ G.} \quad (1)$$

Magnetars are bright thermal X-ray sources, which means that scattering of the thermal X-rays is the dominant source of pair-creating gamma rays. This process has been discussed extensively in the context of radio pulsars, by Kardashev et al. (1984), Daugherty & Harding (1989), Chang (1995), Sturmer 1995), and Hibschan & Arons (2001a,b). Macroscopic electric fields are screened rapidly enough that the electrons and positrons in the inner magnetosphere do not reach the energies that are required for gamma ray emission by curvature radiation. The electrostatic gap model investigated by Hibschan & Arons (2001a,b) and by Thompson (2008) has this property, as does the more dynamic circuit model described in this paper.

We assume that the target X-rays are approximately described by a Planck spectrum with temperature T_{bb} , that is, by a spectrum with an exponential cutoff at $\hbar\omega_X \gg 3k_B T_{bb}$. This assumption is consistent with measurements of the X-ray spectrum of XTE J1810–197 (Halpern & Gotthelf 2005; Gotthelf & Halpern 2005). The spectra of other, brighter, magnetars have a significant tail at 1–10 keV, well above the typical $k_B T_{bb} = 0.4$ keV. However, this tail is likely generated at larger radii (Thompson et al. 2002; Lyutikov & Gavriil 2006; Fernández & Thompson 2007) and diluted near the star compared with the thermal radiation from the star surface.

Denote the angle of photon propagation with respect to \mathbf{B} by θ_{kB} and let $\mu = \cos \theta_{kB}$. For definiteness, let us assume that the magnetic field is predominantly radial near the star. The stellar radiation at a radius r occupies the range of angles $\mu_{\min} \leq \mu \leq 1$ where

$$\mu_{\min}(r) = \left(1 - \frac{R_{NS}^2}{r^2}\right)^{1/2}. \quad (2)$$

and R_{NS} is the stellar radius. We neglect here the effects of gravitational light bending. The energy $\hbar\omega$ of a target photon is

Doppler-boosted in the rest frame of the electron to

$$\hbar\omega' = \gamma(1 - \beta\mu)\hbar\omega. \quad (3)$$

In this frame, the target photon is strongly aberrated and moves nearly parallel to \mathbf{B} .

The scattering cross section is strongly enhanced when the electron is promoted to its first Landau state. The resonant frequency¹ in the electron rest frame is (e.g. Herold 1979)

$$\omega' = \frac{eB}{m_e c}. \quad (4)$$

This translates into a condition on the energy of target photons in the lab frame, which we write as

$$\tilde{\omega} \equiv \frac{\hbar\omega}{k_B T_{\text{bb}}} = \frac{B/B_Q}{\Theta_{\text{bb}} \gamma(1 - \beta\mu)}, \quad (5)$$

where

$$\Theta_{\text{bb}} \equiv \frac{k_B T_{\text{bb}}}{m_e c^2} \quad (6)$$

is the dimensional temperature of the stellar radiation. Setting $\beta = 1$ is a good approximation if the resonant scattering occurs close to the star, where $\hbar eB/m_e c \gg k_B T_{\text{bb}}$.

The target photons move nearly parallel to \mathbf{B} in the rest frame of the scattering particle. For the cross section calculation, one can adopt the description of resonant scattering as absorption followed by de-excitation. Then the cross section is given by (Daugherty & Ventura 1978),

$$\sigma_{\text{res}} = \sigma_{\text{res}}^0 \omega' \delta(\omega' - \omega_B) = \sigma_{\text{res}}^0 \omega \delta\left[\omega - \frac{\omega_B}{\gamma(1 - \mu)}\right], \quad (7)$$

where $\omega_B = eB/m_e c$ and

$$\sigma_{\text{res}}^0 = \frac{2\pi^2 e}{B}. \quad (8)$$

The magnitude of the scattering cross section integrated through the resonance is

$$\langle \sigma_{\text{res}} \rangle \sim \sigma_{\text{res}}^0 \sim \frac{3\pi}{4\alpha_f} \left(\frac{B}{B_Q}\right)^{-1} \sigma_T \gg \sigma_T, \quad (9)$$

where $\alpha_f \simeq 1/137$ is the fine structure constant. Note that σ_{res} is much larger than the Thomson cross section σ_T even in a $\sim 10^{15}$ G magnetic field. By comparison, the cross section below the resonance is strongly suppressed,

$$\sigma^{\text{non-res}} \sim \frac{\sigma_T}{\gamma^2}. \quad (10)$$

The two expressions here apply to both X-ray polarization eigenmodes. These modes are linearly polarized close to the star, where vacuum polarization effects dominate the dielectric properties of the medium.

The rate of resonant scattering is high over a broad range of particle kinetic energies, due to the broad band nature of the black body radiation field. An electron moving radially away from the star with a Lorentz factor $\gamma_{\triangleright} \gg 1$ scatters the thermal X-rays at the rate

$$\Gamma_{\triangleright}^{\text{res}} = \int d\omega \int_{\mu_{\text{min}}}^1 2\pi d\mu \frac{I_\omega}{\hbar\omega} (1 - \mu) \sigma_{\text{res}}(\omega, \mu, \gamma_{\triangleright}), \quad (11)$$

where σ_{res} is the scattering cross section, and I_ω is the spectral intensity of thermal X-rays,

$$I_\omega = \frac{(k_B T_{\text{bb}})^3}{8\pi^3 c^2 \hbar^2} f(\tilde{\omega}), \quad (12)$$

$$f(\tilde{\omega}) = \frac{\tilde{\omega}^3}{e^{\tilde{\omega}} - 1}, \quad \tilde{\omega} \equiv \frac{\hbar\omega}{k_B T_{\text{bb}}}. \quad (13)$$

We count only one polarization mode in I_ω as is appropriate to thermal emission from a strongly magnetized neutron star (e.g. Silantev & Iakovlev 1980).

In the case of an outgoing electron near the neutron star surface, the double integral in equation (11) then yields (Sturmer 1995)

$$\Gamma_{\triangleright}^{\text{res}} = \frac{\alpha_f \Theta_{\text{bb}}^3}{2(B/B_Q)} (1 - \mu_{\text{min}})^2 \tilde{\omega}_{\triangleright}^2 \left| \ln(1 - e^{-\tilde{\omega}_{\triangleright}}) \right| \frac{c}{\lambda_e}, \quad (14)$$

¹ The resonant frequency is given by the non-relativistic cyclotron formula even in super-QED magnetic fields, because the absorbing charge experiences a recoil along \mathbf{B} . Note also that a photon incident along the magnetic field can be resonantly scattered only at a single frequency, corresponding to the transition between the lowest and the first Landau states. Resonant interactions involving higher Landau states drop out for zero inclination angle.

where

$$\tilde{\omega}_{\triangleright}(\gamma_{\triangleright}) \equiv \frac{\hbar\omega}{k_B T_{bb}} = \frac{B/B_Q}{\gamma_{\triangleright} \Theta_{bb}(1-\mu_{\min})}, \quad (15)$$

and γ_{\triangleright} is the Lorentz factor of the scattering charge, $\alpha_f = e^2/\hbar c$ is the fine structure constant, and $\lambda_e = \hbar/m_e c$. The electron resonantly scatters soft X-rays from the Rayleigh-Jeans tail of the spectrum when its Lorentz factor is higher than

$$\gamma_{\triangleright}^{\ominus} \equiv \frac{B/B_Q}{(1-\mu_{\min})\Theta_{bb}} = 2.3 \times 10^4 \frac{B_{15}}{1-\mu_{\min}} \left(\frac{k_B T_{bb}}{0.5 \text{ keV}} \right)^{-1}. \quad (16)$$

The corresponding expression for an ingoing charge is

$$\Gamma_{\triangleleft}^{\text{res}} = \frac{\alpha_f \Theta_{bb}^3}{B/B_Q} (1-\mu_{\min}) f(\tilde{\omega}_{\triangleleft}) \frac{c}{\lambda_e}, \quad (17)$$

where

$$\tilde{\omega}_{\triangleleft} = \frac{\hbar\omega_X}{k_B T_{bb}} = \frac{B/B_Q}{2\Theta_{bb}\gamma_{\text{res}}} = 1.2 \times 10^4 \frac{B_{15}}{\gamma_{\text{res}}} \left(\frac{k_B T_{bb}}{0.5 \text{ keV}} \right)^{-1} \quad (18)$$

and we have made the approximation $r \gg R_{\text{NS}}$.

2.1. Direct Conversion of Gamma-Rays to Pairs

Once created in an ultra-strong magnetic field, a gamma ray will rapidly convert to e^{\pm} pairs. The details of this process depend sensitively on the strength of the magnetic field. The interval between gamma ray emission and pair creation is shortened substantially if the gamma ray is created above the threshold energy for pair creation. Photons this energetic are created by resonant scattering if the magnetic field is stronger than a threshold value, and are always created at some finite rate by non-resonant scattering. We call this process ‘‘direct’’ pair creation to distinguish it from the adiabatic conversion process.

Resonant scattering may be viewed as an excitation of particle to the first Landau level followed immediately by de-excitation. The energy of the scattered photon depends on its pitch angle with respect to the magnetic field, . It is convenient to view this process in the frame where the intermediate (excited) electron does not move along \mathbf{B} . In this frame, the energy of scattered photon is given by (Beloborodov & Thompson 2007),

$$E_{\gamma}() = \frac{E_B}{\sin^2} \left[1 - \left(\cos^2 + \frac{m_e^2 c^4}{E_B^2} \sin^2 \right)^{1/2} \right], \quad (19)$$

where E_B is the energy of the first Landau level,

$$E_B = \left(1 + 2 \frac{B}{B_Q} \right)^{1/2} m_e c^2. \quad (20)$$

The scattered photon will directly convert to an e^{\pm} pair if its energy exceeds the threshold

$$E_{\gamma} > E_{\text{thr}} = \frac{2m_e c^2}{\sin}. \quad (21)$$

Photons scattered with $\theta = \pi/2$ have the minimum $E_{\text{thr}} = 2m_e c^2$ and the maximum $E_{\gamma} = E_B - m_e c^2$ (because the de-exciting electron experiences no recoil). The condition $E_{\gamma} > E_{\text{thr}}$ is satisfied in a range of angles if $E_B - m_e c^2 > 2m_e c^2$, which is equivalent to $B > 4B_Q$. If the surface magnetic field is stronger than this, a large fraction of resonantly scattered photons will directly convert to e^{\pm} near the surface. There is, of course, no constraint on the magnetic field for direct pair creation via non-resonant scattering.

2.2. Adiabatic Conversion of a Single Gamma Ray to an Electron-Positron Pair

A gamma-ray that is formed with an energy $\hbar\omega \gg 2m_e c^2$ and pitch angle $\theta_{kB} \ll 2m_e c^2/\hbar\omega$ is initially below threshold for pair creation, but can propagate through the curved magnetic field to a position where the condition (21) is satisfied (Sturrock 1971). This process is familiar from models of ordinary pulsars with fields $B_{\text{NS}} = 10^{12} - 10^{13}$ G. Pair creation by a single photon can occur just above the threshold energy (21) only if the magnetic field exceeds a minimum strength,

$$B \simeq \frac{4B_Q}{3 \ln[0.2\alpha_{\text{em}} \theta_{kB} (rm_e c/\hbar)]} = 0.05 B_Q \simeq 2 \times 10^{12} \text{ G}. \quad (22)$$

(e.g. Erber 1966; Berestetskii et al. 1982). The corresponding maximum radius for the creation of a pair in the lowest Landau state is

$$\frac{R_{\gamma \rightarrow e^{\pm}}}{R_{\text{NS}}} \simeq 8 B_{\text{NS},15}^{1/3}. \quad (23)$$

Pair creation by energetic photons, $E_{\gamma} \gg 2m_e c^2$, can occur above threshold in weaker magnetic fields, which leads to the emission of multiple synchrotron photons.

In somewhat stronger magnetic fields, the gamma-ray is energetically favored to convert to bound positronium. We highlight here some ambiguities in the existing treatments of this process (Wunner et al 1985; Shabad & Usov 1986) when $B \gtrsim B_Q$. The associated refractive effects have been studied by Shabad & Usov (1984), who argue that the group velocity of the gamma ray will bend and asymptote to the local magnetic field. The perpendicular energy $\hbar\omega \sin\theta_{kB}$ would, in the process, become very close to $2m_e c^2$. Qualitatively, a gamma ray that enters the dispersive regime at $\hbar k_\perp \sim 2m_e c$ can be viewed as a mixture of a pure electromagnetic mode (a photon) and a second mode (an electron-positron pair) that does not propagate across the magnetic field.

The dispersion relation of the gamma ray receives a divergent correction from vacuum polarization near the threshold for pair creation. Neglecting the interaction between the electron and positron, one finds (Shabad & Usov 1984)

$$\omega^2 = c^2 k^2 - 2\alpha_f \left(\frac{B}{B_Q} \right) \exp \left[\frac{-(k_\perp c / \omega_m)^2}{2(B/B_Q)} \right] \frac{\omega_m^3}{(4\omega_m^2 - \omega^2 + c^2 k_\parallel^2)^{1/2}}, \quad (24)$$

where $\omega_m \equiv m_e c^2 / \hbar = 2\pi c / \lambda_e$. This dispersion relation applies to the two polarization modes which are luminal at low and high frequencies, and correspond to a propagating O-mode photon. The lower branch bends over from $\omega \simeq ck$ at small momentum, to $\omega \simeq m_e c^2 / \hbar$ when $k_\perp \gtrsim m_e c / \hbar$.

The electrostatic force between the electron and positron will reduce the energy threshold for pair creation,

$$E_{\text{thr}} \rightarrow \frac{2m_e c^2 - E_{\text{bind}}(k_\perp, B)}{\sin\theta_{kB}}. \quad (25)$$

The binding energy E_{bind} of a positronium atom deviates significantly from the zero-field value $\frac{1}{2} \times 13.6$ eV when $B > B_{\text{atomic}} = \alpha_{\text{em}}^2 B_Q = 2.3 \times 10^9$ G,

$$E_{\text{bind}} \simeq \frac{7}{96} \alpha_{\text{em}}^2 m_e c^2 \ln^2 \left[\frac{B/B_{\text{atomic}}}{1 + (B/B_Q)^{-1} (\hbar k_\perp / m_e c)^2} \right] \quad (26)$$

(Wunner & Herold 1979; Shabad & Usov 1986; Lieb et al. 1992). The effect of this interaction on the gamma ray dispersion curve have been analyzed by Wunner et al. (1985) and Shabad & Usov (1985) by calculating the vacuum polarization using the positive energy wave functions of the bound electron and positron in the magnetic field.

There are, however, some ambiguities in this procedure when $B > B_Q$. First, the dispersion curve (24) deviates strongly from that of a pure photon at the wavenumber $k_\perp = 2m_e c / \hbar$. Writing $\hbar\omega = 2m_e c^2 - \Delta E$ on the lower branch, one finds

$$\frac{\Delta E}{2m_e c^2} \simeq \frac{1}{8} \left(2\alpha_f \frac{B}{B_Q} \right)^{2/3} \exp \left[-\frac{4}{3(B/B_Q)} \right]. \quad (27)$$

One notices that ΔE has a strong exponential dependence on \mathbf{B} , whereas E_{bind} varies only logarithmically. In an ordinary pulsar-strength magnetic field, e.g. $B = 4 \times 10^{12}$ G, equation (27) gives $\Delta E = 6 \times 10^{-4}$ eV, much smaller than the positronium binding energy of ~ 100 eV. The electron-positron interaction is clearly important in this case, and the adiabatic conversion to a bound positronium atom is very plausible. In a super-QED magnetic field, the energy shift ΔE is much larger than the positronium binding energy as calculated from eq. (26): one finds $\Delta E = 15$ keV when $B = 4B_Q$. The energy levels of bound positronium, as calculated in the Bethe-Salpeter approximation, do not show the same distortion when $\hbar k_\perp \simeq 2m_e c$ (Shabad & Usov 1986).

Second, the propagation of a positronium atom in a curving magnetic field is qualitatively different from that of a photon. This process is allowed kinematically because the generalized momentum of each charged particle contains a term $e\mathbf{A}/c$, where $\mathbf{A} = \frac{1}{2}\mathbf{B} \times \mathbf{r}$ is the background vector potential and \mathbf{r} is the displacement from the center of mass. The conservation of momentum perpendicular to \mathbf{B} gives

$$\hbar \mathbf{k}_\perp = \frac{1}{2} \sum_{\alpha=1}^2 e_\alpha (\mathbf{B} \times \mathbf{r}_\alpha), \quad (28)$$

where α labels the electron and positron ($e_1 = -e$, $e_2 = +e$).

As the atom moves away from the star, the electron and positron are individually guided by the magnetic field and the perpendicular momentum of the atom *decreases*: equation (28) implies $k_\perp \sim eB\Delta r_\perp \propto B^{1/2}$. By contrast, the perpendicular wavevector of a photon generally increases as the photon propagates through an inhomogeneous magnetic field: the geometrical optics equations imply that \mathbf{k} is essentially constant (even as the group velocity of the photon becomes aligned with the magnetic field).

And, third, a direct calculation of the coulomb correction to the vacuum polarization gives the same dependence on B (Padden 1994) only if $B < B_Q$.

In the absence of sufficiently high flux of target X-rays, the conversion of a gamma ray to bound positronium remains plausible, because ΔE decreases rapidly as k_\perp rises above $2m_e c / \hbar$. Once formed, a positronium atom can be dissociated by the resonant scattering of an ambient X-ray at a Landau resonance of the electron or positron (§2.3); or by the photoelectric absorption of an ambient IR photon (§2.4). A positronium atom in its ground state is not able to decay into two photons for a simple kinematic reason (Shabad & Usov 1982). The photon dispersion curve $\omega(k_\perp)$ flattens near $k_\perp = 2m_e c / \hbar$, which means that the conservation of momentum perpendicular to \mathbf{B} is not consistent with² conservation of energy: two daughter photons with a total energy $2m_e c^2 - E_{\text{bind}}$ must have a smaller momentum than was contained in the atom.

² In other words, photon splitting is not facilitated by strong dispersion near the threshold for pair creation.

2.3. Disintegration of a Positronium Atom through Absorption of an X-ray at the Electron/Positron Landau Resonance

Given the ambiguities just mentioned in the dispersive properties of the hybrid photon-pair, we approach the problem of pair formation in two ways. The hybrid particle is treated either as a pure photon, or a pure positronium atom, and the relevant pair creation channels are analyzed. A gamma ray can collide with an ambient X-ray while it is still in the mixed state. We find that the cross section for such a two photon collision is resonantly enhanced when the gamma ray by itself is close to the threshold for pair conversion (§3).

Although a positronium atom is electrically neutral, the electron and positron can scatter high-frequency photons whose wavelength is smaller than the electron-positron separation. The minimum separation is set by the transverse momentum of the atom: $\Delta r_{\perp} \simeq \hbar k_{\perp} c / eB$. A single electron at rest will resonantly absorb a photon of energy $(B/B_Q)m_e c^2$ with a cross section (7). The corresponding photon wavelength λ is

$$\frac{\lambda}{\Delta r_{\perp}} = \frac{1}{2} \left(\frac{\hbar k_{\perp}}{2m_e c} \right)^{-1}. \quad (29)$$

We can therefore expect an X-ray photon to be absorbed by either the electron or positron with a cross section close to (7). The photon imparts a recoil momentum to the absorbing particle, which is $\Delta p \sim (B/B_Q)m_e c$ when $B < B_Q$. The atom is dissociated if $(\Delta p)^2/2m_e \gtrsim E_{\text{bind}}$, which requires $B > 1 \times 10^{12}$ G. Because bound pair creation occurs only for magnetic fields stronger than $B > 2 \times 10^{12}$ G $\sim 0.05 B_Q$, dissociation can be assumed to follow immediately following the resonant absorption of the X-ray.

A positronium atom therefore has a very short mean free path for dissociation close to an X-ray bright magnetar. If the original gamma ray is created by resonant scattering of an X-ray by an electron of Lorentz factor γ , then the gamma ray has an energy $\simeq f_{\text{recoil}} \gamma m_e c^2$, where the recoil factor is $f_{\text{recoil}} = \frac{2}{3}$ when $B = 4B_Q$ and $f_{\text{recoil}} \simeq B/B_Q$ for $B \ll B_Q$. The resultant positronium atom has a Lorentz factor $\gamma_{\pm} \simeq (f_{\text{recoil}}/2)\gamma$. The original seed photon for scattering, and the photon that dissociates the positronium atom, therefore tend to be drawn from different parts of the thermal X-ray peak. When $B \gtrsim B_Q$, the photons which act as seeds for pair creation come from above the black body peak, the dissociating photon comes from close to the peak, and the positronium is rapidly dissociated. On the other hand, when $B < B_Q$, the dissociating photon is drawn from the Rayleigh-Jeans tail and, if $k_B T_{\text{bb}}$ is below a critical value, it is possible for a newly created positronium atom to avoid dissociation by resonant scattering. In this circumstance the circuit voltage could be regulated by a different pair-creation channel – such as the direction conversion of non-resonantly scattered photons to pairs (Thompson 2008) – even though the creation rate of gamma rays by resonant scattering were formally higher.

2.4. Photodisintegration of Parapositronium

Many magnetars are intense sources of optical-IR photons, with a characteristic luminosity of 10^{32} ergs s^{-1} (Durant & van Kerkwijk 2006a,b, and references therein). These photons are in the right frequency range to dissociate bound positronium (parapositronium) when the relativistic motion of the bound pairs along \mathbf{B} is taken into account. The binding energy is $E_0 \simeq 200$ eV in a magnetic field $B \sim 4B_Q$ when the threshold for pair creation is $\hbar k_{\perp} = 2m_e c / \hbar$ (eq. [26]). Pair-creating gamma rays typically have energies $\hbar\omega \sim (0.05 - 1)\gamma_{\text{p}}^{\ominus} m_e c^2$ near the surface of the star, depending on the details of the circuit model (Thompson 2008). The resulting pair has a Lorentz factor $\gamma = \hbar\omega / 2m_e c^2 \sim (500 - 10^4) B_{15} (k_B T_{\text{bb}} / 0.5 \text{ keV})^{-1}$ parallel to \mathbf{B} (see eq. [16]). Photons of an energy

$$\hbar\omega \simeq \frac{E_0}{\gamma(1-\mu_{\text{min}})} \sim (0.02 - 0.4) B_{15}^{-1} \left(\frac{k_B T_{\text{bb}}}{0.5 \text{ keV}} \right) \text{ eV} \quad (30)$$

will be most effective at photodissociating positronium.

The cross section for photodissociation is suppressed compared with an unmagnetized positronium atom (see, e.g., Fig. 1 of Potekhin & Pavlov 1997). The photon is incident along \mathbf{B} in the rest frame of the atom, and so both (linear) polarization modes have nearly identical cross sections. However, the motion of the charges in the atom is restricted in the plane perpendicular to \mathbf{B} , and the cross-sectional area of the atom is reduced by a factor

$$\begin{aligned} a_B^{-2} \left(\frac{eB}{\hbar c} \right)^{-1} &= \left(\frac{B}{B_{\text{atomic}}} \right)^{-1} \\ &= \frac{\alpha_{\text{em}}^2}{16} \left(\frac{B}{4B_Q} \right)^{-1} = 3.3 \times 10^{-6} \left(\frac{B}{4B_Q} \right)^{-1}. \end{aligned} \quad (31)$$

Here $a_B = 2\hbar^2 / m_e e^2$ is the Bohr radius of an unmagnetized positronium atom, and

$$B_{\text{atomic}} = \frac{1}{4} \alpha_{\text{em}}^2 B_Q = 6 \times 10^8 \text{ G} \quad (32)$$

is the magnetic field that begins to significantly deform the atom away from its unmagnetized structure.

The cross section for a photon incident parallel to \mathbf{B} with an energy just above the threshold E_0 can be estimated as

$$\sigma_{\text{phot}}(\omega') \sim \frac{\pi^2 e^2}{(m_e/2)(E_0/\hbar)c} \left(\frac{B}{B_{\text{atomic}}} \right)^{-1}, \quad (33)$$

where $m_e/2$ is the reduced mass. (See Potekhin & Pavlov 1997 for more detailed expressions.) The rate of photodissociation in response to a spectral intensity I_ω of optical-IR photons is

$$\Gamma_{\text{phot}} = \int d\omega \int_{\mu_{\min}}^1 2\pi d\mu (1-\mu) \frac{I_\omega}{\hbar\omega} \sigma_{\text{phot}}(\omega'), \quad (34)$$

as measured in the frame of the star.

We now show that photodissociation is rapid if the optical-IR continuum of a magnetar is emitted close to its surface. In evaluating the above integral, we also make use of the observation that the luminosity density L_ω is roughly independent of frequency in at least some AXP sources. Then

$$\Gamma_{\text{phot}} = (1-\mu_{\min}) \frac{\pi e^2 L_\omega}{4r^2 m_e c |E_0|} \left(\frac{B}{B_{\text{atomic}}} \right)^{-1}, \quad (35)$$

where $L_\omega/4\pi r^2 = 2\pi I_\omega(1-\mu_{\min})$. It is convenient to express Γ_{phot} in terms of the luminosity ωL_ω at $\hbar\omega = 0.1$ eV. Approximating $1-\mu_{\min} \simeq \frac{1}{2}(r/R_{\text{NS}})^{-2}$, and re-expressing r in terms of the local value of the magnetic field, gives

$$\Gamma_{\text{phot}} = 1 \times 10^7 \frac{(\omega L_\omega)_{32}}{B_{\text{NS},15}^{4/3} R_{\text{NS},6}^2} \left(\frac{B}{4B_Q} \right)^{1/3} \text{ s}^{-1}. \quad (36)$$

We see that photodissociation is rapid, $\Gamma_{\text{phot}} > c/R_{\text{NS}}$, if the surface luminosity at 0.1 eV is higher than $\sim 10^{29}$ ergs s⁻¹. This critical luminosity is only $\sim 10^{-2}$ – 10^{-3} of the typical K-band luminosities of AXPs; but it is also $\sim 10^6$ times *larger* than expected from the Rayleigh-Jeans tail of the X-ray black body. Photodissociation of positronium could therefore be slow if the optical-IR output were concentrated at a greater distance from the star. For example, a very dense pair gas forms on the open magnetic field lines in the circuit model described in §4. The pair density is high enough to seed the optical-IR emission of the transient magnetar XTE J1810–197 by a form of plasma emission (Thompson 2008). In that case, the optical-IR flux would be beamed away from the star, and from the base of the open magnetic flux tube.

3. COLLISIONS BETWEEN GAMMA RAYS AND THERMAL X-RAYS

High-energy photons can create pairs by colliding with thermal X-rays. This pair creation channel is important when the X-ray flux is high (e.g. Zhang & Qiao 1998). Although most gamma rays will first convert to pairs off the magnetic field, a significant amount of pair creation by photon collisions may take place within a gap. If the surface temperature of the neutron star is higher than $\sim kT_{\text{bb}} = 0.2$ keV, then the gap voltage is reduced.

We consider the collision between a gamma ray and a thermal X-ray that is emitted directly from the magnetar surface,

$$\gamma + X \rightarrow e^+ + e^-. \quad (37)$$

The gamma ray is created with an energy³ $\omega \gg 2m_e$, but below the threshold for single-photon pair creation, $\omega \sin \theta_{kB} < 2m_e$. At the point of pair creation, it is nearly completely polarized in the ordinary mode, due to the rapid splitting of extraordinary mode gamma rays. The target photon has an energy $\omega_X \ll m_e$. The kinematic threshold for pair creation through the channel (37) is obtained from the equations of conservation of energy and momentum parallel to \mathbf{B} ,

$$\begin{aligned} \omega + \omega_X &= (P_+^2 + m_e^2)^{1/2} + (P_-^2 + m_e^2 + 2neB)^{1/2}; \\ \mu\omega + \mu_X\omega_X &= P_+ + P_-, \end{aligned} \quad (38)$$

where $\mu = \cos \theta_{kB}$, $\mu_X = \cos \theta_{kB,X}$ are the direction cosines of the gamma ray and X-ray, and P_\pm are the momenta of the final electron and positron. One finds

$$2\omega\omega_X(1-\mu\mu_X) > (m_e + E_{0n})^2 - \omega^2(1-\mu^2), \quad (39)$$

where $E_{0n} = (m_e^2 + 2neB)^{1/2}$ and $\omega(1-\mu^2)^{1/2} = \omega \sin \theta_{kB}$ is the perpendicular energy of the gamma ray.

Two particular cases are of interest here:

1. — The gamma-ray remains well below the threshold for pair creation, $\omega(1-\mu^2)^{1/2} \ll 2m_e$, so that vacuum polarization effects introduce very little dispersion into the relation between ω and k . The target photon is tightly collimated about \mathbf{B} in the frame where the net momentum of the two photons along \mathbf{B} vanishes ($\theta'_{kB,X} \sim 2m_e c^2/\hbar\omega$; Fig. 1). Pair creation with the both final particles in Landau state $n = 0$ has the same threshold condition

$$\omega\omega_X(1-\mu_X) = 2m_e^2, \quad (40)$$

where we have set $\mu \simeq 1$. This is identical to the threshold condition in the absence of a magnetic field.

We have evaluated the cross section for this process to the lowest order in perturbation theory. The tree-level Feynman diagrams are calculated using wavefunctions for the electron and positron that are good spin eigenstates (Melrose & Parle 1983a,b). Details

³ In this section, we employ natural units in which $\hbar = c = 1$.

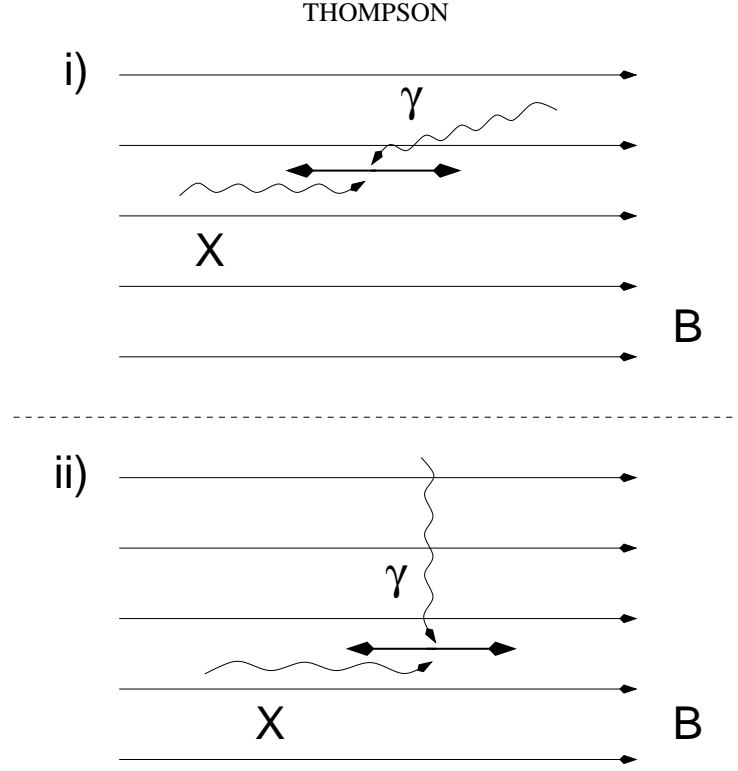


FIG. 1.— Collision of a gamma ray with a target X-ray. We consider two cases: i) the collision occurs close to the point of emission of the gamma ray, so that the gamma ray is well below the threshold for single photon pair creation ($\hbar\omega \sin \theta_{kB} \ll 2m_e c^2$); and ii) the gamma ray is just below threshold (eq. [43]). In case i) the two photons move nearly head on in the center-of-momentum frame parallel to \mathbf{B} . In case ii), the cross section is strongly enhanced if the target photon has an energy $\sim (B/B_Q)m_e c^2$ in the frame where the gamma ray moves perpendicular to \mathbf{B} .

are provided in the Appendix. We find

$$\left(\frac{V_{\pm}}{c}\right) \sigma_{X\gamma} = \frac{3\sigma_T}{16} \left(\frac{B}{B_Q}\right) \left(\frac{E_{\pm}}{m_e}\right)^{-2} \left| \frac{\varepsilon_2^+ \varepsilon_1^- m_e^2}{(E_{\pm} + P_{\pm})^2 + m_e^2 + 2eB} - \frac{\varepsilon_1^+ \varepsilon_2^- m_e^2}{(E_{\pm} - P_{\pm})^2 + m_e^2 + 2eB} \right|^2, \quad (41)$$

where E_{\pm} and $P_{\pm} = P_- = -P_+$ are energy and momenta of the outgoing electron and positron (both in the lowest Landau state) in the center-of-momentum frame, and $V_{\pm} = |P_{\pm}|/E_{\pm}$. The polarization vectors of the two colliding photons in this frame are denoted by $\varepsilon_k^{\pm} = \varepsilon_k^x \pm i\varepsilon_k^y$. Expression (41) simplifies to

$$\left(\frac{V_{\pm}}{c}\right) \sigma_{X\gamma} = \frac{3\sigma_T}{16} \frac{B/B_Q}{(1+B/B_Q)^2} (\varepsilon_1^y \varepsilon_2^x - \varepsilon_2^y \varepsilon_1^x)^2 \quad (V_{\pm} \ll c) \quad (42)$$

near threshold. The coefficient works out to $0.03\sigma_T$ in a magnetic field $B = 4B_Q$. This result differs somewhat in the dependence on B and the numerical coefficients from those of Kozlenkov & Mitrofanov (1986), who used the wavefunctions for the Dirac particles that are not good spin eigenstates and did not explicitly evaluate the polarization dependence.

2. — The gamma-ray is just below the threshold for pair creation,

$$\omega(1-\mu^2)^{1/2} = 2m_e - \Delta E. \quad (43)$$

In the case of adiabatic conversion of a gamma ray to a pair, ΔE measures the amount by which the dispersion curve of the photon bends below the rest energy of an electron-positron pair. For example, $\Delta E \simeq 15$ keV when the perpendicular momentum of the photon is $k_{\perp} = 2m_e$ in a magnetic field $B = 4B_Q$ (eq. [27]).

In this situation, there is a very low threshold energy for the creation of a pair with both particles in Landau level $n = 0$. Transforming to the frame⁴ in which the gamma ray moves perpendicular to \mathbf{B} , one has

$$\omega'_X > \Delta E. \quad (44)$$

This energy is even smaller in the stellar frame, $\omega_X = \omega'_X/\gamma(1-\mu_X)$. When one of the final state particles is in a higher Landau state n , one obtains

$$\omega'_X = \Delta E + \frac{1}{2} \left(n \frac{eB}{m_e} + E_{0n} - m_e \right), \quad (45)$$

⁴ Obtained by a boost with Lorentz factor $\gamma = 1/\sin \theta_{kB} \simeq 2m_e/\Delta E$ along \mathbf{B} .

which reduces to $\Delta E + eB/m_e$ in a sub-QED magnetic field.

The cross section is strongly enhanced if the virtual electron that mediates the collision between the two photons is on mass shell. This is possible only if the energy of the target X-ray satisfies a resonance condition. (The main difference with the resonance encountered in cyclotron scattering is that the virtual electron can remain in the lowest Landau state.) We take the gamma ray (parallel momentum $\mu'\omega' = 0$) to share a vertex with the outgoing positron (see Fig. 4). The parallel momentum P'_l of the virtual electron is related to that of the target X-ray ($\mu'_X\omega'_X \simeq \omega'_X$) and final-state electron by

$$P'_l = -\omega'_X + P'_- = -P'_+. \quad (46)$$

The resonance conditions are⁵

$$(\omega'_X - E'_-)^2 = (\omega' - E'_+)^2 = P'^2 + m_e^2. \quad (47)$$

We are searching for the lowest-energy resonance, and so take the virtual electron to be in the lowest Landau level. The condition of energy conservation

$$\omega' + \omega'_X = E'_+ + E'_- \quad (48)$$

is satisfied only if one final particle is in the lowest Landau state, e.g. $n_+ = 0$. Then the solution to equations (46), (47) is

$$E'_+ = m_e \quad E'_- = \omega'_X \left(1 + \frac{m_e^2}{2n_- eB} \right) + n_- \frac{eB}{2\omega'_X}, \quad (49)$$

where we have approximated $\omega' \simeq 2m_e$. Applying eq. (48) shows that the energy of the target X-ray must satisfy the same resonance condition as for absorption by a real charge at its first Landau transition,

$$\omega'_X = \gamma(1 - \mu_X)\omega_X = n_- \frac{eB}{m_e c}. \quad (n_- > 0). \quad (50)$$

The resonant target photon energy is essentially the same as the threshold energy (45) when $B < B_Q$, but lies substantially above threshold in super-QED magnetic fields.

It should be emphasized that this resonance is only approximate when $\Delta E > 0$. Substituting $n_+ = 0$ into eq. (49), one sees that

$$E'_+ = m_e - \frac{1}{2}\Delta E. \quad (51)$$

A true resonance is not possible, because one particle in the final state would not be able to satisfy the mass shell condition. But an approximate resonance is present when $\Delta E \ll 2m_e$. The cross section derived in the Appendix is

$$\frac{\sigma}{\sigma_T} = \frac{3}{8} e^{-2B_Q/B} \left(\frac{m_e}{\omega' - 2E'_+} \right)^2 (\varepsilon^z)^2. \quad (52)$$

In this expression, the frequency ω' and polarization ε^z of the incident gamma ray, and the energy E'_+ of the outgoing positron, are evaluated in the frame where the gamma ray perpendicular to **B**.

The momentum of the positron can be evaluated in terms of the displacement of the energies of the gamma ray and target photon from the resonant values $\omega' = 2m_e$ and $\omega'_X = eB/m_e$:

$$\left(\frac{B}{B_Q} \right) P'_+ = \left(1 + \frac{B}{B_Q} \right) (2m_e - \omega') + \omega'_X - \frac{eB}{m_e}. \quad (53)$$

The cross section peaks at $P'_+ = 0$, where the denominator of eq. (52) has the minimum value ΔE^2 .

The cross section exhibits additional localized peaks where the energy threshold for excitation to higher Landau levels is just satisfied (Kozlenkov & Mitrofanov 1986). We ignore this effect in this paper, being interested in the case where the fluxes of gamma rays and target X-rays are both cut off exponentially at high frequencies.

4. HIGH PAIR DENSITIES IN A TURBULENT FLUX ROPE

A twisted magnetosphere is subject to current-driven instabilities, which can drive fluctuations in the twist and facilitate its redistribution across magnetic flux surfaces. Before considering the time evolution of the twist in §5, we first consider the influence that these twist fluctuations would have on the pair density in the outer magnetosphere. We describe a novel state for the open-field circuit with very strong and efficient particle heating. Pair creation is driven by low-energy particles and is concentrated close to the star, although the heating is distributed over a wide range of radii (see Fig. 2).

Analogous effects are believed to occur in the magnetosphere of one star in the double pulsar system J0737–3039, which is exposed to the relativistic wind of the second, faster pulsar. The dynamic twist can, in both cases, have important consequences for the particle energy distribution in the circuit (Thompson & Blaes 1998; Lyutikov & Thompson 2005). On some flux tubes, the current that is drawn from the surface of the star will intermittently be pushed above $J = \rho_{GJC}$, which has the effect of igniting pair creation in order to supply the charges that are demanded by the circuit.

Yet higher current densities will result from the non-linear coupling between torsional Alfvén waves propagating in opposing directions along the magnetic field, which can create a high-frequency spectrum of modes. The necessary condition for this

⁵ We can equally well exchange the electron and positron in the final state; both Feynman diagrams contribute to the resonant cross section.

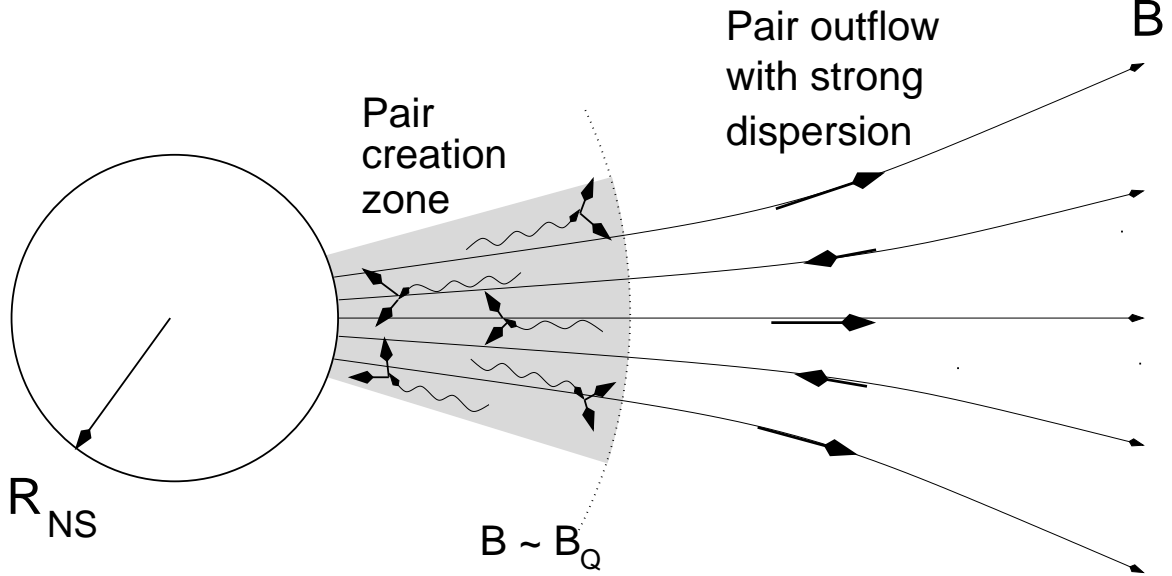


FIG. 2.— The excitation of a torsional wave on the extended magnetic field lines (open and closed) heats the enclosed electrons and protons when the wave energy cascades to a high wavenumber. The fluctuating component of the current diverges in the cascade. There is a critical wavenumber above which the relativistic plasma particles can no longer conduct charge at the rate demanded by the waves, and the wave energy is transferred to the particles. When the particle density is much higher than n_{GJ} and the plasma is nearly charge-balanced, then waves are excited close to the star, where resonantly scattered photons can convert directly to pairs off the magnetic field. The loss of charges from the open magnetic field lines can be balanced by pair creation within the innermost part of the circuit if the spin period is shorter than the critical value given by eq. (79).

cascade to occur is that the magnetic field lines are sheared over a scale (transverse to the magnetic field) that is somewhat smaller than the radius. The cascade is not restricted to the closed magnetic field lines, since an outgoing wave is supplied by reflection from the surface of the star.

Consider a torsional wave of a moderate amplitude

$$\delta B_\phi(r, t) \sim B_\phi \quad (54)$$

which propagates along the dipolar magnetic field $B = B_{NS}(r/R_{NS})^{-3}$. Here

$$B_\phi = \left(\frac{J}{\rho_{GJ}c} \right) \left(\frac{\Omega r}{c} \right)^{3/2} B(r) \quad (55)$$

is the static toroidal field at an angle $\theta \sim \theta_{\text{open}}$ from the magnetic axis, where

$$\theta_{\text{open}}(r) = \left(\frac{\Omega r}{c} \right)^{1/2} \quad (56)$$

is the polar angle subtended by the open bundle of magnetic field lines. In addition, J is the current density that is drawn from the surface of the star along the open field lines, $\rho_{GJ} = -\mathbf{\Omega} \cdot \mathbf{B}/2\pi c$ is the corotation charge density (Goldreich & Julian 1969), and $\mathbf{\Omega}$ is the spin vector of the star. The wave is decomposed into ingoing and outgoing components,

$$\delta B_\phi(r, t) = \delta B_\phi^-(r + V_w t) + \delta B_\phi^+(r - V_w t) \quad (57)$$

which move with a phase speed V_w close to the speed of light. We are interested in the case where the charged particles that support the wave have a one-dimensional relativistic distribution, which extends up to some Lorentz factor γ_{max} . Then

$$\frac{V_w}{c} = \frac{\omega}{k_\parallel c} = \left(1 + \frac{1}{\sigma} \right)^{1/2} \left(1 + \frac{k_\perp^2 c^2}{4\gamma_{\text{max}}^2 \omega_p^2} \right)^{-1/2}. \quad (58)$$

In this expression, $\omega_p = (4\pi n_\pm e^2/m_e)^{1/2}$ is the non-relativistic plasma frequency, and $\sigma \simeq B^2/8\pi\gamma_{\text{max}} n_\pm m_e c^2$.

The coupling parameter that determines the strength of the interaction between two colliding Alfvén waves is $k_\perp \xi_\phi = k_\perp \delta B_\phi / k_\parallel B$, where ξ_ϕ is the rotational displacement of the magnetic field lines and k_\perp and k_\parallel are the components of the wavevector perpendicular to and parallel to \mathbf{B} . A cascade develops if the shear of the field lines at the forcing scale is stronger than

$$k_{\perp,0} \gtrsim \frac{2\pi}{\theta_{\text{open}} r} \left(\frac{\delta B_{\phi,0}}{B_\phi} \right)^{-1}. \quad (59)$$

Here $\delta B_{\phi 0}$ is the r.m.s toroidal field at the forcing scale, which is take to be

$$\frac{2\pi}{k_{\parallel}} = L \sim \frac{cP}{2\pi}. \quad (60)$$

This coupling parameter has been hypothesized to be regulated to $k_{\perp} \xi_{\phi} \sim 1$ throughout the inertial range of the wave spectrum (Goldreich & Sridhar 1995). Then a wavepacket undergoes a significant distortion during a single collision. If the cascade is characterized by a constant flux of energy toward higher wavenumbers,

$$\frac{dU_{\text{cas}}}{dt} \sim \frac{\delta B_{\phi}^2}{8\pi} k_{\parallel} c = \text{const}, \quad (61)$$

then the Alfvén wavepackets become increasingly elongated within the inertial range, $k_{\perp} \propto k_{\parallel}^{3/2}$.

The fluctuation in the current density associated with the Alfvén waves increases in magnitude toward higher wavenumbers,

$$\delta J = \frac{c}{4\pi} k_{\perp} \delta B_{\phi} \propto k_{\perp}^{2/3}, \quad (62)$$

whereas the energy density in the toroidal field fluctuation decreases,

$$\frac{\delta B_{\phi}^2}{8\pi} = \frac{\delta B_{\phi 0}^2}{8\pi} \left(\frac{k_{\parallel} L}{2\pi} \right)^{-1}. \quad (63)$$

The current fluctuations at the damping scale are therefore much larger than the mean current density. When the plasma is cold, the damping scale is obtained by balancing the r.m.s. current density of the wave with the maximum conduction current that the plasma can supply,

$$k_{\perp} \delta B_{\phi} \sim 4\pi e n_{\pm}. \quad (64)$$

The inner scale of the turbulent spectrum therefore sits at a wavenumber $k_{\parallel, \text{max}} \sim 4\pi e n_{\pm} / B$.

We are, however, interested in the case where the plasma is dilute enough that the charges become relativistic. The heated charges are assumed to move only in the direction parallel to \mathbf{B} . This assumption is well justified close to the star, where we focus our attention, due to the rapidity of synchrotron cooling. In this case, the particles that support the fluctuating component of the current must reverse direction: the current fluctuation due to charges that do not reverse direction is negligible, because their velocity undergoes only a small change, $\delta v \sim c/\gamma^2$. We deduce that the current fluctuation is supported by only a fraction of the heated charges, with a net density $\delta n_{\pm} < n_{\pm}$, and a characteristic Lorentz factor γ_{damp} that is smaller than the mean Lorentz factor $\langle \gamma \rangle \sim \delta B_{\phi 0}^2 / 8\pi n_{\pm} m_e c^2$. The associated damping scale is given by

$$k_{\parallel, \text{max}} \sim \frac{4\pi e \delta n_{\pm}}{B}. \quad (65)$$

It turns out to be possible to deduce δn_{\pm} and the damping scale without knowing the distribution function of the charges in detail. At the damping scale, the energy ΔE_{damp} deposited per charge in one wave period is comparable to the kinetic energy $\gamma_{\text{damp}} m_e c^2$ of the charges that reverse direction,

$$\Delta E_{\text{damp}} \sim \frac{1}{\delta n_{\pm}} \frac{dU_{\text{cas}}}{dt} \frac{2\pi}{k_{\parallel, \text{max}} c} \sim \gamma_{\text{damp}} m_e c^2. \quad (66)$$

Here

$$\frac{dU_{\text{cas}}}{dt} \sim \Omega \frac{\delta B_{\phi 0}^2}{8\pi}. \quad (67)$$

(Except for the primary Goldreich-Julian charge flow, higher-energy particles come in pairs of opposite signs that do not gain or lose a significant amount of energy.) Combining eqs. (65) - (67) then gives the damping scale

$$k_{\parallel, \text{max}} \sim \frac{2\pi}{R_{\text{NS}}} \left(\frac{8\pi^2 e B_{\text{NS}} R_{\text{NS}}}{\gamma_{\text{damp}} m_e c^2} \right)^{1/2} \left(\frac{\Omega R_{\text{NS}}}{c} \right)^2, \quad (68)$$

where B_{NS} is the polar magnetic field strength. The values of γ_{damp} and $k_{\parallel, \text{max}}$ can be determined independently by the physics of pair creation, which leads to a constraint on the spin period (§4.1).

A comment about Landau damping is in order here. We are interested in the regime where the fluctuating component of the twist is comparable to the mean twist, so that $\sigma \sim 1$. The Alfvén waves then resonate only with the low-energy tail of the particle distribution, and the Landau damping time is much longer than the wave period. Since the lifetime of a wavepacket is comparable to the wave period in a critically balanced cascade, the effects of Landau damping can be neglected. As a result, Landau damping of the Alfvén waves is ineffective and the inner scale of a turbulent spectrum is located at the scale where the waves become charge starved.⁶

⁶ See Thompson (2006) for a description of the conditions in which these two damping regimes will be found in a cold plasma.

4.1. Maximum Spin Period for High Rates of Pair Creation

We now consider the range of spin periods and dipolar magnetic fields that can support rapid pair creation with the circuit model just described. We focus on the resonant scattering of thermal X-rays by relativistic charges, which requires only modest particle energies and can therefore be effective at high particle densities. The creation of pair-creating gamma rays by this process is, however, only effective within a relatively small distance from the star.

The rate of energy deposition by a turbulent cascade is conveniently normalized to the corotation particle density $n_{\text{GJ}} = \Omega B / 2\pi e c$, so that $(1/n_{\text{GJ}})dU_{\text{cas}}/dt$ is approximately independent of radius. If pair creation is concentrated close to the star, then $n_{\pm} \propto n_{\text{GJ}} \propto r^{-3}$ on the open magnetic field lines, and the heating rate per electron or positron will be approximately constant. Heating is cut off inside a minimum radius

$$R_{\text{min}} \sim \frac{1}{k_{\parallel, \text{max}}} \ll \frac{c}{\Omega}, \quad (69)$$

where the energy density in the fluctuating toroidal field becomes small, $\delta B_{\phi}^2 / 8\pi \propto r^2$.

An upper bound on R_{min} is obtained by requiring that the magnetic field be strong enough for pair creation. One therefore requires a short damping scale and a high pair multiplicity. If the spin frequency of the star is too low, then the damping energy ΔE_{damp} becomes too small for the heated particles to produce pair-creating gamma rays. The energy threshold for pair creation is lower for ingoing charges, for which the resonance condition (3) is most easily satisfied. We therefore focus on pair creation by photons that are resonantly scattered toward the star.

Pairs that are created by this process can be supplied to the outer magnetosphere only if they reverse direction, that is, only if their kinetic energy is smaller than $\Delta E_{\text{damp}} = \gamma_{\text{damp}} m_e c^2$ (eq. [66]). The energy of a resonantly scattered photon can be related to the kinetic energy $\gamma_{\text{res}} m_e c^2$ of the scattering charge via

$$E_{\gamma} = f_{\text{recoil}} \gamma_{\text{res}} m_e c^2 \simeq \left(\frac{B}{B_{\text{Q}}} \right) \gamma_{\text{res}} m_e c^2. \quad (70)$$

(It will turn out that pair creation is concentrated where $B < B_{\text{Q}}$, and so we approximate $f_{\text{recoil}} \sim B/B_{\text{Q}}$.) The energy of the gamma ray is approximately divided in two by pair creation, which leads to the relation

$$\gamma_{\text{damp}} = \frac{B(R_{\text{min}})}{2B_{\text{Q}}} \gamma_{\text{res}}. \quad (71)$$

Pair creation in the zone $r \sim R_{\text{min}}$ will balance the loss of charges from the circuit if γ_{res} (and therefore the energy ΔE_{damp}) exceeds a critical value. The resonant scattering rate (17) depends exponentially on γ_{res} when the target photon is drawn from the high-energy tail of the black body distribution. The value of γ_{res} that yields a significant rate of resonant scattering decreases as one moves away from the star, but its value at a fixed radius depends only logarithmically on the pair creation rate through the parameter $\tilde{\omega}_{\triangleleft}$ (eq. [18])

$$\gamma_{\text{res}} = \frac{B(R_{\text{min}})/B_{\text{Q}}}{2\tilde{\omega}_{\triangleleft}\Theta_{\text{bb}}}. \quad (72)$$

One requires $\tilde{\omega}_{\triangleleft} \simeq 12$ if n_{\pm}/n_{GJ} is almost uniform throughout the open-field circuit.

The values of R_{min} and γ_{damp} can now be determined by requiring that photons of energy (70) able to convert to pairs off the magnetic field. The corresponding condition is

$$E_{\gamma} \frac{r_{\text{min}}}{R_{\text{C}}(r_{\text{min}})} > 2m_e c^2, \quad (73)$$

where

$$\frac{R_{\text{C}}(r)}{R_{\text{NS}}} = \tilde{\varepsilon}_3^{-1} \left(\frac{r}{R_{\text{NS}}} \right)^3 \quad (74)$$

is the radius of curvature of the field lines, and is assumed to be dominated by the quadrupole/octopole component of the magnetic field [see eq. (A9) of Thompson 2008]. One finds,

$$\frac{R_{\text{min}}}{R_{\text{NS}}} < 3.2 \tilde{\varepsilon}_3^{1/8} B_{\text{NS},15}^{1/4} \left(\frac{\tilde{\omega}_{\triangleleft}}{12} \right)^{-1/8} \left(\frac{k_{\text{B}} T_{\text{bb}}}{0.5 \text{ keV}} \right)^{-1/8}, \quad (75)$$

and

$$B(r_{\text{min}}) > 3.1 \times 10^{13} \tilde{\varepsilon}_3^{-3/8} B_{\text{NS},15}^{1/4} \left(\frac{\tilde{\omega}_{\triangleleft}}{12} \right)^{3/8} \left(\frac{k_{\text{B}} T_{\text{bb}}}{0.5 \text{ keV}} \right)^{3/8} \text{ G}. \quad (76)$$

The corresponding energy of the pair-creating charges is

$$\gamma_{\text{res}} > 30 \tilde{\varepsilon}_3^{-3/8} B_{\text{NS},15}^{1/4} \left(\frac{\tilde{\omega}_{\triangleleft}}{12} \right)^{-5/8} \left(\frac{k_{\text{B}} T_{\text{bb}}}{0.5 \text{ keV}} \right)^{-5/8}, \quad (77)$$

and the energy of the resultant pairs is

$$\gamma_{\text{damp}}(R_{\text{min}}) > 10 B_{\text{NS},15}^{1/2} \tilde{\varepsilon}_3^{-3/4} \left(\frac{\tilde{\omega}_{\triangleleft}}{12} \right)^{-1/4} \left(\frac{k_B T_{\text{bb}}}{0.5 \text{ keV}} \right)^{-1/4}. \quad (78)$$

Charges can be supplied self-consistently to the circuit only if the spin period is shorter than a critical value, which is obtained by substituting expressions (75) and (78) into eq. (69) and then into eq. (68),

$$P < P_{\text{crit}} = 7.7 \tilde{\varepsilon}_3^{1/4} B_{\text{NS},15}^{1/4} R_{\text{NS},6}^{5/4} \text{ s}. \quad (79)$$

When the spin period is larger than (79), the cascade deposits energy too far from the star to deflect ingoing pairs from their creation zone at $r \sim R_{\text{min}}$ back out into the circuit. This expression has the attractive feature of depending only weakly on the polar magnetic field B_{NS} and the degree of curvature of the magnetic field lines; it is also independent of T_{bb} and $\tilde{\omega}_{\triangleleft}$. However, the normalization does depend on the numerical coefficient (eq. [69]) relating the minimum radius for pair creation to the damping scale: one finds $P_{\text{crit}} \propto (k_{\parallel,\text{max}} R_{\text{min}})^{-1/2}$. The electric potential fluctuations at the damping scale will, in practice, have some distribution about $\Delta E_{\text{damp}}/e$ (eq. [66]), with an exponential cutoff at large values. As a result, the supply of pairs to the outer circuit is possible if R_{min} is somewhat smaller than the Alfvén wavelength at the damping scale, as is assumed here.

The charges flowing outward toward the open end of the magnetic flux tube continue to gain energy, because the cascade energy is deposited broadly throughout the circuit. The gamma-ray emitting particles at $r \sim R_{\text{min}}$ have an energy $\gamma_{\text{res}} > \gamma_{\text{damp}}$ (eq. [71]), and therefore have typically been heated at a larger radius and then partially deflected back toward the star. Without prescribing in detail the pair distribution function, it is possible to set a lower bound on the multiplicity in the circuit,

$$\mathcal{M}_{\pm} = \frac{2\pi e n_{\pm} c}{\Omega B} > \frac{2\pi e \delta n_{\pm} c}{\Omega B}. \quad (80)$$

Substituting eqs. (65) and (69), one finds

$$\mathcal{M}_{\pm} > \frac{1}{2} \left(\frac{\Omega R_{\text{min}}}{c} \right)^{-1} = 4 \times 10^3 \tilde{\varepsilon}_3^{-1/8} B_{\text{NS},15}^{-1/4} \left(\frac{P}{6 \text{ s}} \right) \left(\frac{k_B T_{\text{bb}}}{0.5 \text{ keV}} \right)^{1/8}. \quad (81)$$

Given a constant outward flux of pairs with a radial velocity comparable to c , the mean energy per charge is

$$\begin{aligned} \langle \gamma(r) \rangle &\sim \frac{r}{\mathcal{M}_{\pm} n_{\text{GJ}}} \frac{dU_{\text{cas}}}{dt} \\ &< 4 \times 10^4 \tilde{\varepsilon}_3^{-1/8} B_{\text{NS},15}^{5/4} R_{\text{NS},6}^3 \left(\frac{P}{6 \text{ s}} \right)^{-3} \left(\frac{k_B T_{\text{bb}}}{0.5 \text{ keV}} \right)^{-1/8} \left(\frac{\delta B_{\phi,0}}{B_{\phi}} \right)^2 \left(\frac{J}{\rho_{\text{GJ}} c} \right)^2 \left(\frac{r}{L} \right). \end{aligned} \quad (82)$$

Note that $\langle \gamma \rangle > \gamma_{\text{damp}}$ at $r > R_{\text{min}}$: most of the heating is at the low-momentum end of the distribution function $f(P)$. If $df/dP \sim 0$ at low momentum, then $\delta n_{\pm}/n_{\pm} \sim \gamma_{\text{damp}}/\langle \gamma \rangle$. But $\delta n_{\pm} \propto \gamma_{\text{damp}}^{-1/2}$, and so we deduce

$$\gamma_{\text{damp}}(r) = \gamma_{\text{damp}}(R_{\text{min}}) \left(\frac{r}{2\pi R_{\text{min}}} \right)^{2/3}. \quad (83)$$

The damping scale $2\pi/k_{\parallel,\text{max}} \propto \delta n_{\pm}^{-1}$ increases as the $\frac{1}{3}$ power of the radius.

A competing circuit solution that could lead to such large pair multiplicities is an outer gap bounded by the surface $\mathbf{\Omega} \cdot \mathbf{B} = 0$ (Cheng, Ho, & Ruderman 1986; Cheng & Zhang 2001). The voltage across such a gap can approach the total open-field voltage. Seed charges can be created in the gap by collisions between curvature gamma rays and thermal X-rays from the neutron star surface. The energetic charges created in such a gap will, however, be beamed down toward the star, and pair creation will be concentrated in a zone where the open field lines are occulted by the star. Such a voltage structure is therefore not a promising source for the observed emission of the radio magnetars.

5. VARIABILITY IN THE OPEN-FIELD VOLTAGE DUE TO MAGNETOSPHERIC ACTIVITY

The variations in the spindown torque of SGRs and AXPs are remarkable in their amplitude and longevity: the spindown rate is observed to increase smoothly over a period of months, by up to a factor ~ 4 (Kaspi et al. 2001; Woods et al. 2002; Woods et al. 2007; Tam et al. 2007; Camilo et al. 2007a, 2008). The strength of the torque variations correlates roughly with the level of activity that the magnetar has sustained over the preceding years, but this correlation is only indirect. In several cases the torque increase is observed with a delay of months following an episode of X-ray burst activity, and can persist long after the initial active period. The burst emission of SGRs and AXPs is highly intermittent (Woods & Thompson 2006): a nice example is provided by the AXP 1E 2259+586, whose activity as a hard-spectrum X-ray source was localized within a day, and was followed by an extended cooling of the thermal X-ray emission (Woods et al. 2004). In the most active sources, the magnetar can remain in a new spindown state for years at a time, with the torque several times larger than in the preceding state.

Strong variations in spindown torque, extending over a period of at least several months, have also been detected in the radio monitoring of the transient AXP XTE J1810–197 (Camilo et al. 2007b). This torque variability persisted long after the initial X-ray activation (in fact, after the hard-spectrum component of the transient X-ray emission had largely decayed away). Even more

remarkably, the torque increased by at least a factor ~ 3 compared with older X-ray timing data, making the relative increase in the spin down rate comparable to that seen in the most active SGRs.

These torque variations have been interpreted in the magnetar model in terms of a restructuring of the magnetosphere. Two effects have been considered which can increase the open magnetic flux, the open-field current, and the torque acting on the star.

1. – A persistent static twist may be sustained in the closed magnetosphere, driven by the unwinding of an internal toroidal magnetic field (Thompson et al. 2002; Beloborodov & Thompson 2007). In the process, magnetic helicity is expelled from the interior of the star. The twist is stabilized as long as the outward flux of helicity across the outer boundary of the magnetosphere is kept small.

As a dipolar magnetic field is twisted, the poloidal field lines flare out slightly. The large size of the corotating magnetosphere then allows a significant increase in the open-field current. In a first approximation, one additional parameter is introduced into the description of the magnetosphere, namely the twist angle $\Delta\phi$ on the field lines that are anchored near the magnetic poles. In the self-similar construction of Thompson et al. (2002), the radial index of the magnetic field softens from $\mathbf{B} \propto r^{-3}$ to $\mathbf{B} \propto r^{-K}$ with $K < 3$. The angular width of the bundle of open field lines therefore increases from $\theta_{\text{open}}^2 = \Omega r/c$ to⁷

$$\theta_{\text{open}}^2 = \left(\frac{\Omega R_{\text{NS}}}{c} \right)^{K-2} \quad (K < 3). \quad (84)$$

The voltage across the open flux bundle is proportional to θ_{open}^2 . A twist of one radian forces a reduction in K to 2.85 (see Fig. 2 of Thompson et al. 2002). At a fixed rate of spin, the voltage increases by a factor $(cP/2\pi R_{\text{NS}})^{3-K} = 4.7(P/6 \text{ s})^{0.15} R_{\text{NS},6}^{-0.15}$, as does the polar magnetic field that is inferred from the magnetic dipole model.

2. – A persistent relativistic wind is driven by internal seismic activity within the star. This wind combs out the dipolar field lines into a radial configuration in the outer magnetosphere (Thompson & Blaes 1998; Harding et al. 1999; Thompson et al. 2000).

The conversion of internal magnetic and seismic energy to a persistent wind has an uncertain efficiency: it involves the transfer of energy across magnetic flux surfaces from an injection zone situated far inside the speed-of-light cylinder. For example, torsional waves in the outer magnetosphere have a much lower frequency than do internal elastic modes of the neutron star crust: the fundamental toroidal mode of the crust has a period $P_{\text{elastic}} \sim 0.02 \text{ s}$ (Strohmayer et al. 1991) and couples to dipolar field lines with a maximum radius $R_{\text{max}} \sim 0.4 c P_{\text{elastic}}$, only $\sim 10^{-2}(P/6 \text{ s})$ of the light cylinder radius. A wind can therefore be driven by the excitation of waves in the closed magnetosphere, but the power dissipated on field lines that open out across the light cylinder may be only a small fraction of the total.

Measurements of the torque behavior of magnetars offer ways of discriminating between these two models.

A transient twisting up of the magnetic field has the effect of increasing the open-field voltage and reducing the critical spin period below expression (79). If the detection of the radio emission from an individual magnetar typically requires a broad radio beam, and therefore depends on a high pair density on the open field lines (see Thompson 2008), then one can understand why an individual source would become visible as a radio pulsar following a period of X-ray burst activity. Starting with a value of P_{crit} larger than the present spin period, a twisting of the magnetic field can force P_{crit} to a smaller value and ignite a high rate of pair creation on the open field lines.

The delays that are observed between burst activity and torque increases can be interpreted in terms of the resistive evolution of the current within the closed magnetosphere, which has a timescale of $\sim 1 \text{ yr}$ close to the star (Beloborodov & Thompson 2007). Their existence is less clear in the case where the torque change is driven by persistent seismic activity. An attractive feature of the twisted dipole model is that small injections of twist from the neutron star interior can force large structural changes in the outer magnetosphere (where the magnetic field energy is relatively small). Indeed, the energetic output of XTE J1810–197 during its period of X-ray activity was modest by the standards of the Soft Gamma Repeaters; but the amplitude of the subsequent change in spindown torque was as large as is seen in the most active SGRs.

The measured upper bound on the spin periods of magnetars places additional strong constraints on how the magnetosphere is restructured. A persistent wind of particles and Alfvén waves drives an exponential increase in the spin period,

$$\frac{dP}{dt} \simeq \frac{4\mu_{\text{NS}}}{3I_{\text{NS}}} \left(\frac{L_{\text{wind}}}{c} \right)^{1/2} P, \quad (85)$$

where $\mu_{\text{NS}} = \frac{1}{2} B_{\text{NS}} R_{\text{NS}}^3$ is the magnetic moment.⁸ This formula applies when the wind luminosity L_{wind} is much larger than the magnetic dipole luminosity $L_{\text{MDR}} = \frac{2}{3} \mu_{\text{NS}}^3 \Omega^4 / c^3$. One finds

$$\frac{dP/dt|_{\text{wind}}}{dP/dt|_{\text{MDR}}} = 6.0 \frac{L_{\text{wind},35}^{1/2}}{B_{\text{NS},15} R_{\text{NS},6}} \left(\frac{P}{6 \text{ s}} \right)^2. \quad (86)$$

We deduce that a relativistic wind can dominate the spindown torque of a magnetar only rarely — otherwise the spin periods

⁷ This expression is accurate when K is only slightly smaller than 3; it neglects any change in the distribution of flux across the neutron star surface.

⁸ In the case of a centered dipole, μ_{NS} can be related to the polar magnetic field B_{NS} and the average surface field $\langle B_{\text{NS}} \rangle$ via $\mu_{\text{NS}} = \frac{1}{2} B_{\text{NS}} R_{\text{NS}}^3 = \langle B_{\text{NS}} \rangle R_{\text{NS}}^3$. It is $\langle B_{\text{NS}} \rangle$ that is usually quoted in the pulsar literature. Hence a polar magnetic field $B_{\text{NS}} = 10^{15} \text{ G}$, the usual normalization in this paper, corresponds to $\langle B_{\text{NS}} \rangle = 5 \times 10^{14} \text{ G}$ and a magnetic moment $\mu_{\text{NS}} = 5 \times 10^{32} R_{\text{NS},6}^3 \text{ G cm}^3$.

of magnetars should cover a broad range. The efficiency of this torque mechanism does not depend in an obvious way on the spin period and the rate of pair formation the open magnetic field lines. Alfvén waves in the closed magnetosphere are supported by charges particles of both signs, that are drawn directly from a light-element surface layer, or supplied by pair creation near the magnetar surface (as in the circuit model of Beloborodov & Thompson 2007).

5.1. Timescale for Resistive Evolution of the Closed-Field Current and the Open-Field Voltage

Strong variations in radio brightness and pulse shape are detected from the two radio magnetars on timescales of minutes to hours (Camilo et al. 2007b, 2008). These variations have a possible interpretation in terms of the resistive evolution of currents in the outer closed magnetosphere, which drives variations in the open-field voltage.

Let us first consider the gradual redistribution of twist that would result from smooth gradients in the field-aligned voltage across the poloidal flux surfaces. To estimate the timescale in the outer magnetosphere, we consider the power dissipated on field lines that extend to a certain maximum radius R_{\max} . The self-similar model of a twisted magnetosphere described in Thompson et al. (2002) has a current density of the form

$$\mathbf{J} = \alpha \mathbf{B}; \quad \alpha = \frac{c \Delta \phi}{4\pi R_{\text{NS}}} \sin^2 \theta_0. \quad (87)$$

Here θ_0 is the polar angle at which a given field line intersects the star, and $\Delta \phi$ is the net twist angle between the two magnetic footpoints. We assume that $\Delta \phi$ is constant in the outer magnetosphere, although in general it will vary across the poloidal flux surfaces. Then the toroidal magnetic field is given by

$$B_\phi(r, \theta) = \frac{\Delta \phi \sin^3 \theta}{2r^3} \mu_{\text{NS}}, \quad (88)$$

and the net current flowing across a radius $r > R_{\text{NS}}$ is

$$I(> r) = \int_0^{\pi/2} J_r(r, \theta) 2\pi r^2 \sin \theta d\theta = \frac{\Delta \phi}{8} c B_{\text{NS}} R_{\text{NS}} \left(\frac{r}{R_{\text{NS}}} \right)^{-2}. \quad (89)$$

Given that each closed flux surface develops the same voltage Φ_e , the dissipation rate is

$$L_{\text{diss}}(> r) = I(> r) \Phi_e. \quad (90)$$

The decay time of the twist can be deduced from L_{diss} and the energy in the toroidal field, which is

$$E_\phi(> r) \equiv \int_r^\infty r'^2 dr' \int d\Omega \frac{B_\phi^2}{8\pi} = \frac{(\Delta \phi)^2}{210} B_{\text{NS}}^2 R_{\text{NS}}^3 \left(\frac{r}{R_{\text{NS}}} \right)^{-3}. \quad (91)$$

The timescale for the resistive evolution of the twist at radius r is

$$t_{\text{res}}(r) \sim \frac{E_\phi(> r)}{L_{\text{diss}}(> r)} = 0.1 \Delta \phi B_{\text{NS},15} R_{\text{NS},6}^2 \left(\frac{|e\Phi|}{\text{GeV}} \right)^{-1} \left(\frac{P}{6 \text{ s}} \right)^{-1} \left(\frac{r}{R_{\text{lc}}} \right)^{-1} \text{ days}. \quad (92)$$

Here we have normalized r to the light cylinder radius $R_{\text{lc}} = c/\Omega$. The field-aligned voltage Φ is the integral of $-E_{\parallel} = -\mathbf{E} \cdot \hat{\mathbf{B}}$ along a closed magnetic field line between its two footpoints,⁹ The value of Φ in the outer magnetosphere depends on details of the return current toward the star: a gap forming at the surface of an X-ray bright magnetar has a voltage $e\Phi \sim 1$ GeV (Thompson 2008), which is similar to the voltage deduced from the 1-dimensional circuit model of Beloborodov & Thompson (2007). At constant Φ , the resistive timescale increases toward the star.

Our evaluation of t_{res} is 1-2 orders of magnitude longer than the shortest timescale for radio flux variability observed in the magnetars XTE J1810–197 and 1E 1547.0–5408. The underlying voltage fluctuations may therefore be triggered by current-driven instabilities in the outer magnetosphere. In the next section, we consider the origin of these instabilities, and how they are regulated by pair creation.

5.2. Stability of the Magnetospheric Twist

A substantial increase in the open-field current and spindown torque will result from a twisting of the magnetosphere only if the twist is distributed over a broad range of radii. If the twist were concentrated within a distance $\sim 2R_{\text{NS}}$ of the neutron star, the effect would be much more limited. The detection of strong nonthermal X-ray emission from a magnetar does not necessarily imply that the source is in its highest torque state. For example, the AXP 4U 0142+61 is a copious source of 100 keV X-rays (Kuiper et al. 2006), but its characteristic age is relatively long ($t_{\text{sd}} = P/2\dot{P} = 70$ kyr); its outer magnetosphere may therefore be only weakly twisted.

How stable is a magnetosphere with a broadly distributed twist? A self-similar configuration with a constant value of the twist angle is not in its minimum-energy (‘Taylor-relaxed’) state. The constant of proportionality α between the current density \mathbf{J} and magnetic flux density \mathbf{B} varies with position (eq. [87]). In particular, it depends on the polar angle θ_0 at which a given field line

⁹ This quantity represents the line integral of $(1/c)dA_{\parallel}/dt$ – not the change in the scalar potential, which must vanish given the high electrical conductivity of the neutron star.

intersects the star, which provides a convenient label for the poloidal flux surfaces. In what follows, we allow $\Delta\phi$ to be a function of θ_0 .

Such a configuration with α decreasing toward the magnetic symmetry axis is susceptible to redistribution of twist into the outer magnetosphere. The kinetic energy of the charges that supply the closed-field current is small compared with the magnetic energy, which means that the magnetosphere is nearly force free. The energy of a force-free magnetic field is minimized at constant α (Woltjer 1958). When $\Delta\phi$ is constant, most of the magnetic helicity is stored in the inner magnetosphere:

$$\mathcal{H}(r) \sim [\pi r^2 B_P(r)]^2 \Delta\phi(r) \propto \frac{\Phi(r)}{r^2}. \quad (93)$$

The same is true when α is constant: in this case $\Delta\phi \propto 1/\sin^2\theta_0 \propto r$, and $\mathcal{H} \propto r^{-1}$. The toroidal field energy is therefore minimized when most of the helicity is concentrated close to the neutron star. At the same time, the redistribution of a small portion of the helicity into the outer magnetosphere can drive the twist angle to large values.

To describe the stability properties of the magnetosphere in more detail, it is useful to define appropriate angular coordinates. We focus on axisymmetric equilibria, for which the magnetic field can be written as

$$\mathbf{B} = \mathbf{B}_P + \mathbf{B}_\phi = \nabla\Psi_P \times \nabla\left(\frac{\phi}{2\pi}\right) + \nabla\Psi_\phi \times \nabla\left(\frac{\eta}{2\pi}\right). \quad (94)$$

Here $\Psi_P = \mu_{\text{NS}} \sin^2\theta/r$ is the flux coordinate for a dipolar magnetic field, and $\nabla\phi = \hat{\phi}/r \sin\theta$ in spherical coordinates (r, θ, ϕ) . The toroidal magnetic field corresponding to eq. (87) is given by eq. (88). The toroidal flux threading a poloidal flux surface of cross-section S that is anchored at angle θ_0 is

$$\Psi_\phi(\theta_0) = \int_S r dr d\theta B_\phi(r, \theta). \quad (95)$$

The surface integral (95) can be transformed into an integral over θ and θ_0 using the relation $r = R_{\text{NS}} \sin^2\theta / \sin^2\theta_0$,

$$\Psi_\phi(\theta_0) = \frac{\Delta\phi \mu_{\text{NS}}}{R_{\text{NS}}} \int_{\theta_0}^{\pi/2} \sin\theta'_0 \cos\theta'_0 d\theta'_0 \int_{\theta'_0}^{\pi-\theta'_0} \sin\theta d\theta. \quad (96)$$

The distribution of toroidal flux with surface polar angle is

$$\frac{d\Psi_\phi}{d\sin\theta_0} = \frac{2\Delta\phi \mu_{\text{NS}}}{R_{\text{NS}}} \sin\theta_0 \cos\theta_0, \quad (97)$$

and the dual angular variable is

$$\frac{\eta}{2\pi} = \frac{1}{2} \left(1 - \frac{\cos\theta}{\cos\theta_0} \right). \quad (98)$$

The strength of the winding in the magnetosphere can be described in terms of the relative periodicities in the ϕ and η directions,

$$\frac{1}{q(\theta_0)} \equiv \frac{d\phi}{d\eta} = \frac{B_\phi}{B_\theta \sin\theta} \left(\frac{d\eta}{d\theta} \right)^{-1} = \frac{\Delta\phi(\theta_0)}{2\pi} \cos\theta_0. \quad (99)$$

A twisted magnetic field is subject to a variety of current-driven instabilities. Ideal MHD instabilities set in at strong values of the twist: the kink instability is present when the ‘safety factor’ $q \leq 1$ in cylindrical geometry (e.g. Wesson 2004). On the other hand, the flaring of the dipolar magnetic field lines has a strong effect on the spindown torque even when $\Delta\phi \simeq 0.5 - 1$, which corresponds to $q \simeq 5 - 10$. The hard X-ray emission of magnetars can be powered by even weaker twists in the inner magnetosphere: only $\Delta\phi \sim 0.1$ is required (Thompson & Beloborodov 2005, Beloborodov & Thompson 2007), corresponding to $q \sim 10^2$.

The redistribution of twist by tearing instabilities within the closed magnetosphere of a neutron star must therefore be considered. Resistive kink instabilities are known to trigger a redistribution of current across magnetic flux surfaces in tokamak plasmas. They can be excited at lower values of the twist, and are sensitive to the current distribution within the tokamak torus.¹⁰

Here there is an important distinction between a tokamak plasma and the twisted magnetosphere of a neutron star. The toroidal current in a tokamak plasma torus is observed to relax rapidly to a constant- α state if the current is concentrated initially near the outer boundary of the torus. As a result, the profiles of the current and the safety factor q both become much flatter in near the long axis of the torus (Fig. 3a,b). The outer magnetosphere of a neutron star can, by contrast, sustain a current distribution in which the q -profile is flat across the poloidal flux surfaces ($\Delta\phi$ is constant) even though the current density decreases toward the magnetic axis, $J \propto \theta^2$ (Fig. 3c).

¹⁰ Our notation here is the inverse of that in the tokamak literature: the unstable component of the twist is in the azimuthal direction ϕ , whereas in a toroidal tokamak plasma it is in the θ direction. The poloidal magnetic field of a neutron star is supported by currents embedded in the star, and the external toroidal field by currents flowing through the magnetospheric plasma. In the case of a tokamak, the toroidal magnetic field is supported by external currents that loop around the long axis of the torus, and the poloidal field (B_θ) is supported by plasma currents.

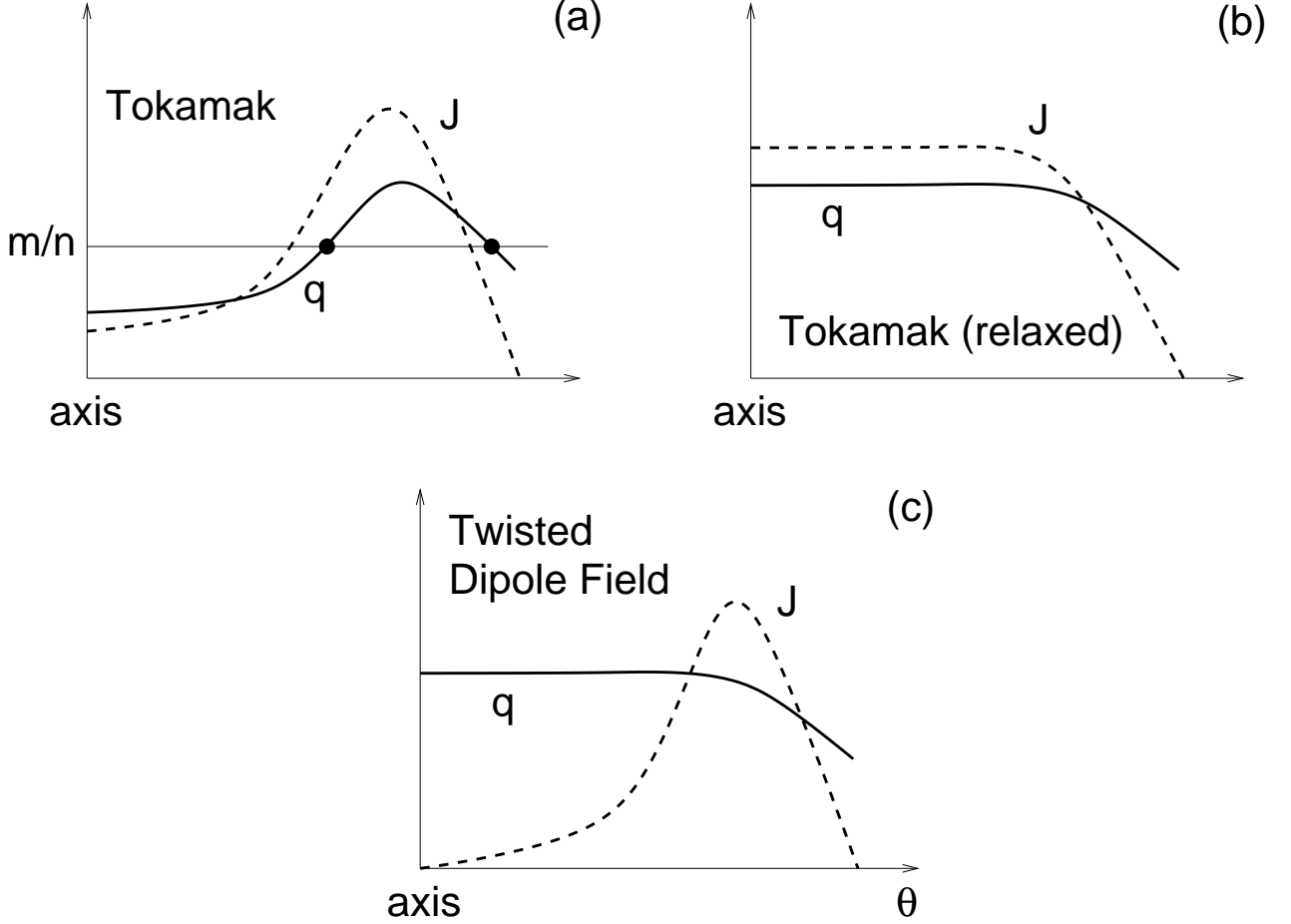


FIG. 3.— Cross section of the current density J and safety factor q in a plane perpendicular to the long axis of a tokamak torus (panels a,b) and to the symmetry axis of a twisted dipole magnetic field (panel c). In a tokamak, q must have a minimum near the axis if J does. A given mode then can interact with two rational surfaces, which accentuates the growth rate of current sheets at the rational surfaces. The net effect is a rapid flattening of the current and safety factor profiles. By contrast, the q profile can remain quite flat near the symmetry axis in a neutron star magnetosphere, even though J has a minimum on the axis.

This difference in the shape of the q -profiles in unrelaxed tokamak and neutron star plasmas has interesting implications for the excitation of resistive kink instabilities. The tearing modes which facilitate the redistribution of twist across the (toroidal) flux surfaces are concentrated on rational surfaces where

$$(\mathbf{B} \cdot \nabla) \delta \mathbf{J} = \frac{iB_\phi}{R} \left(\frac{m}{q} - n \right) \delta \mathbf{J} = 0. \quad (100)$$

Here $\delta \mathbf{J} \propto e^{i(m\theta - n\phi)}$ is the current perturbation and R is the large radius of the plasma torus. The analogous form for the current perturbation in a neutron star magnetosphere is

$$\delta \mathbf{J} \propto \exp \left[im\phi - i\pi n \left(1 - \frac{\cos \theta}{\cos \theta_0} \right) \right], \quad (101)$$

where the roles of the θ and ϕ angular variables are reversed. It is straightforward to check that

$$(\mathbf{B} \cdot \nabla) \delta \mathbf{J} = \frac{iB_\theta}{r} \left(\frac{\Delta \phi}{2\pi} m - n \right) \delta \mathbf{J}, \quad (102)$$

where we have set $\cos \theta_0 \rightarrow 1$ for the most extended dipole field lines.

When the current distribution across the long axis of a tokamak torus has a localized maximum, then so does the distribution of q . As a result, a single resonance $q = m/n$ can appear at two separate surfaces within the torus (Fig. 3). These double tearing modes appear to be important in the process of Taylor relaxation (e.g. Stix 1976). They can be avoided in the twisted magnetosphere of a neutron star if the twist has the same sign on the open and closed magnetic field lines in both magnetic hemispheres. The presence of a highly conducting boundary also tends to suppress tearing modes at rational surfaces near the outer boundary of tokamak plasmas (e.g. Wesson 2004).

The spin of the star induces a twist on the open magnetic field lines with the same sign as the twist that is sustained by the outward Goldreich-Julian current. A reversal in the sign of the twist on the open field lines, if sustained over many rotation

periods, therefore demands a reversal in the sign of the conduction current. This is possible only if a polarizable plasma is present on the open field lines: the space charge density on the open magnetic field lines just above the surface of the neutron star must be the same as ρ_{GJ} . On this basis, Thompson et al. (2002) conjectured that the rate of reconnection near the magnetospheric boundary would be sensitive to the pair production rate in the open-field accelerator.

The stability of the twist in the outer magnetosphere depends on whether the safety factor q (eq. [99]) can maintain a flat profile across the open-field boundary. In the standard pulsar model, the open-field current in each hemisphere is compensated by a return current of the same magnitude that flows along a narrow annulus of closed field lines just inside the magnetospheric boundary. If the open-field current had the opposite sign to the Goldreich-Julian current in one hemisphere, then the toroidal field would go to zero on the flux surface bounding the return current sheath. This would have the effect of allowing double rational surfaces to form, in close analogy with a Tokamak plasma (Fig. 3). By contrast, when the open-field current is able to reverse sign, then the q -profile can remain flat and double rational surfaces do not form.

6. CLUSTERING OF SPIN PERIODS IN THE MAGNETAR POPULATION AND THE SUDDEN BRIGHTENING OF RADIO MAGNETARS

X-ray bright magnetars¹¹ range in spin periods between 0.33 and 11.8 seconds. The upper cutoff to the spin distribution is statistically significant (Psaltis & Miller 2002). The distribution is also quite strongly peaked: removing two sources (1E 1547.0–5408, $P = 2$ s, and PSR J1846–0258, $P = 0.33$ s), the remaining spin periods lie between 5.2 and 11.8 s. If the stars underwent simple magnetic dipole spindown, then a range of 2.3 (6) in spin period would correspond to a range of ~ 5 (~ 30) in age. The measured characteristic ages actually have a much wider distribution, from several hundred years in the most active SGRs to 2×10^5 yrs in the AXP 1E 2259+586. The observation of strong fluctuations in spindown torque in individual sources shows that part of the dispersion in characteristic ages is due to variations in magnetospheric structure. This measured torque variability cannot be related a narrowing of the spin period distribution unless the underlying mechanism is sensitive to the rate of pair creation in the outer magnetosphere.

We are interested in the case where the rate of injection of toroidal field energy into the inner magnetosphere (when averaged over the episodes of X-ray activity) is much higher than the spindown power. The net twist on the magnetic field lines that thread the closed magnetosphere and the interior of the star can be described by the magnetic helicity $\mathcal{H} = \int \mathbf{A} \cdot \mathbf{B} dV$, where \mathbf{A} is the vector potential. The toroidal magnetic field in the closed magnetosphere is susceptible to reconnection with the external magnetic field. We explained in §5.2 how this process could be impeded by a high rate of pair creation on the open magnetic field lines (see also Thompson et al. 2002).

A slow loss of helicity across the outer boundary of the closed magnetosphere can force large-amplitude fluctuations in the twist on the open magnetic field lines, and reverse its sign in one hemisphere. The required rate of loss is

$$\left. \frac{d\mathcal{H}}{dt} \right|_{\text{lc}} \simeq - [\pi R_{\text{lc}}^2 B_P(R_{\text{lc}})]^2 \Omega, \quad (103)$$

where $R_{\text{lc}} = cP/2\pi = 3 \times 10^5 (P/6 \text{ s})$ km. The corresponding damping time of the twist $\Delta\phi$ close to the star is therefore

$$\frac{\Delta\phi(r)}{|d\Delta\phi(r)/dt|_{\text{lc}}} \simeq 30 \frac{\Delta\phi}{R_{\text{NS},6}} \left(\frac{P}{6 \text{ s}} \right)^3 \text{ yr}. \quad (104)$$

In the case of a magnetar, the damping time in the inner magnetosphere is comparable to the resistive decay time of several years (eq. [92]).

We have shown in §4 that a very high pair density can be sustained in the outer magnetosphere if a dynamic twist is excited and then damped through a turbulent cascade to high spatial wavenumbers. This process depends on a high rate of particle heating close to the star, where the rate of resonant scattering is high, and the resonantly scattered photons are energetic enough to convert to pairs. The critical spin period P_{crit} (eq. [79]) for such a gas to be sustained on the open magnetic field lines is several seconds, and depends weakly on the polar magnetic field strength and the curvature of the open magnetic field lines.

6.1. Metastable Twisted Magnetosphere and Torque Decay

We are led to conjecture that the outer magnetosphere can enter a metastable state in which the twist is lost across the magnetospheric boundary at a controlled rate, just high enough to excite large fluctuations in the twist over a single rotation of the star. This metastable state depends on the presence of a dense pair gas in the outer magnetosphere, which can limit the rate of reconnection of the closed magnetosphere with the open-field bundle. The detection of hard X-ray emission at a level $L_X \simeq 10^{35}$ ergs s^{-1} from AXPs with little known X-ray burst activity (Kuiper et al. 2004, 2006) leads to the remarkable inference that magnetic helicity can be stored in the magnetosphere for several years. Hard X-ray emission of a comparable luminosity has been detected from SGR 1900+14 in a relatively quiescent state, nearly a decade after the last major X-ray burst activity (Götz et al. 2006b). Very bright emission ($\sim 10^{36}$ ergs s^{-1}) was detected from SGR 1806–20 by Integral within two years of its major 2004 outburst (Mereghetti et al. 2005).

The observed peak in the distribution of magnetar spins can then be explained if most of the spindown torque is accumulated in this metastable, twisted state, and not when the magnetosphere is more nearly dipolar. Once the spin period of the star grows beyond the value (79), the magnetosphere cannot sustain the inflated, twisted state. Of course, there is some hysteresis in this

¹¹ Observed with persistent luminosities of 10^{35} erg s^{-1} or above over a period of years or decades. See the McGill Magnetar web page for an up-to-date list of magnetar properties; <http://www.physics.mcgill.ca/~pulsar/magnetar/main.html>.

process, because a high rate of pair creation can be reignited by the process of twisting (§5), but this only introduces a spread of a factor ~ 2 in the value of P_{crit} . We also emphasize that this does not exclude an important contribution of a particle wind to the torque when the outer magnetosphere is nearly dipolar (Spitkovsky 2006).

We must therefore examine whether most of the spindown can realistically occur when the magnetosphere is twisted. The duty cycle of the magnetospheric twist can be determined by combining the magnetospheric dissipation rate (which can be measured in the hard X-ray band) with net twist of the internal magnetic field. The internal field cannot be directly measured, but the energetics of the giant flares of the SGRs point to the presence of internal magnetic fields approaching 10^{16} G (e.g. Hurley et al. 2005).

We suppose that, on multiple occasions, a certain amount of helicity is injected into the magnetosphere due to the release of sub-surface stresses, and is stored there. The decay time of the twist can be deduced from eq. (92), by substituting explicitly for the magnetospheric dissipation rate L_{diss} ,

$$\begin{aligned} t_{\text{decay}} &= \frac{E_\phi}{L_{\text{diss}}} = \frac{32}{105} \frac{L_{\text{diss}} R_{\text{NS}}}{c^2 \Phi_e^2} \\ &= 0.1 L_{\text{diss},35} R_{\text{NS},6} \left(\frac{\Phi_e}{10^9 \text{ V}} \right)^{-2} \text{ yr.} \end{aligned} \quad (105)$$

If the current is concentrated on poloidal field lines that are anchored within an angle $\theta < \theta_c$ of the magnetic axis, then it is easy to show that $L_{\text{diss}} \propto \theta_c^4$ and $t_{\text{decay}} \propto \theta_c^2$.

The net duration t_{twist} of the twisted state in the magnetosphere is determined by the winding angle $\Delta\phi_i$ of the internal magnetic field. Given that a toroidal magnetic field is present to a depth ΔR below the stellar surface, one has $\Delta\phi_i \sim (\Delta R/R_{\text{NS}}) B_{\phi,i}/B_{\text{NS}}$ and

$$\begin{aligned} t_{\text{twist}} &\simeq \frac{\Delta\phi_i}{\Delta\phi} t_{\text{decay}} = \frac{4}{105} \frac{B_{\phi,i} R_{\text{NS}} \Delta R}{\Phi_e c} \\ &= 120 R_{\text{NS},6}^2 \left(\frac{B_{\phi,i}}{10^{16} \text{ G}} \right) \left(\frac{\Phi_e}{10^9 \text{ V}} \right)^{-1} \left(\frac{\Delta R}{R_{\text{NS}}} \right) \text{ yr.} \end{aligned} \quad (106)$$

The spindown rate of the magnetar is accelerated when its magnetosphere is twisted. We define

$$(\dot{\nu})_{\Delta\phi} = N_b \dot{\nu}_0, \quad (107)$$

where $\dot{\nu}_0$ is the frequency derivative in the absence of twisting. The acceleration factor is quite large, $N_b \sim 10$, if the twist angle is as large as 1 radian (Thompson et al. 2002), but observations suggest $N_b \lesssim 4$. Given that t_{twist} is smaller than the total age¹² $t_{\text{sd},0}$ of the magnetar, the relative frequency change due to spindown in the twisted and untwisted states is

$$\frac{(\Delta\nu)_{\Delta\phi}}{(\Delta\nu)_0} = N_b \frac{t_{\text{twist}}}{t_{\text{sd},0}}. \quad (108)$$

Consider an SGR with an observed spindown age $t_{\text{sd},0}/N_b = 200$ yrs, which is the minimal value obtained from the spin monitoring of SGR 1806-20 (Woods et al. 2007). Most of the spindown will occur in the twisted state, $(\Delta\nu)_{\Delta\phi} > (\Delta\nu)_0$, if

$$\left(\frac{B_{\phi,i}}{10^{16} \text{ G}} \right) \left(\frac{\Phi_e}{10^9 \text{ V}} \right)^{-1} \left(\frac{\Delta R}{R_{\text{NS}}} \right) > 1.7, \quad (109)$$

and if the loss of helicity due to non-axisymmetric instabilities in the magnetosphere can be neglected in comparison with ohmic damping in situ. If the voltage is as small as $\sim 10^8$ V, then twisting of the magnetosphere can continue to enhance the time-averaged torque as long as the spindown age is shorter than $\sim 10^4$ yrs.

6.2. Torque Decay due to Dipole-Spin Axis Alignment?

In this picture, the spin evolution of magnetars is driven by departures from a dipole structure in the closed magnetosphere. The limiting spin period for magnetars is then not directly tied to the radio death line of pulsars. We should, nonetheless, consider seriously the possibility that an active pair accelerator has been entirely quenched on the open magnetic field lines of many magnetars. X-ray pulse measurements of magnetars would then provide valuable information about the electrodynamic properties of pulsars on both sides of the radio death line.

This intriguing possibility encounters two basic difficulties. First, pair creation by the resonant scattering of thermal X-rays is very effective near the X-ray bright surface of a magnetar, and a pair discharge can be maintained on the open magnetic field lines at spin periods significantly longer than the observed range of magnetars (e.g. Medin & Lai 2007). Second, a reduction in the open-field particle luminosity would result in a large reduction in torque only if the magnetic dipole and rotation axes were nearly aligned, so that the magnetic dipole luminosity in vacuum is much smaller than the particle luminosity in the active state (e.g. Contopoulos & Spitkovsky 2006).

¹² We neglect any departures from a simple magnetic dipole torque model, except for those due to twisting. Thompson et al. (2002) found that the braking index $n = \dot{\nu}\nu/(\dot{\nu})^2$ is slightly smaller than the dipole value ($n = 3$) in the twisted state, but this feature is not important for present purposes.

Observations of PSR B1931+24, which undergoes radio nulls of a month-long duration, show the torque is reduced by a factor $\sim \frac{2}{3}$ when the radio emission is off (Rea et al. 2006). If $\boldsymbol{\mu}$ and $\boldsymbol{\Omega}$ are inclined by an angle χ_{1931} in this object, then one deduces that the ratio of magnetic dipole luminosity to particle luminosity is, more generally,

$$\frac{L_{\text{MDR}}}{L_{\text{particle}}} \simeq 2 \frac{\sin^2 \chi}{\sin^2 \chi_{1931}} \quad (110)$$

in a radio-bright state. The characteristic age of the AXP 1E 2259+586 is $\sim 2 \times 10^5$ yrs, some 20 times longer than the estimated age of the surrounding supernova remnant CTB 109 (Sasaki et al. 2004). To explain a reduction of a factor ~ 20 in torque following the quenching of radio emission, one would require that $\sin^2 \chi < \sin^2 \chi_{1931}/40$.

There are strong arguments against the alignment of $\boldsymbol{\mu}$ and $\boldsymbol{\Omega}$ in most magnetars. The rotational bulge of a slowly rotating magnetar is much smaller in amplitude than the variation in the lengths of the principal axes due to the internal magnetic field. When the internal field is predominantly toroidal, the star becomes prolate in shape and its two largest principal moments of inertia lie in the plane perpendicular to the magnetic symmetry axis. The star reaches a state of minimum rotational energy (at fixed spin angular momentum) when $\boldsymbol{\Omega}$ lies in this plane (e.g. Cutler 2002). If the external magnetic moment were aligned with the symmetry axis of the internal field, then there would be no reason to expect alignment between $\boldsymbol{\mu}$ and $\boldsymbol{\Omega}$.

A near alignment between $\boldsymbol{\mu}$ and $\boldsymbol{\Omega}$ would be easier if the magnetic moment were distributed randomly with respect to the axis of the internal toroidal field. But in that case, the probability of finding alignment to the degree of precision required for 1E 2259+586 is only $\frac{1}{2}\chi^2 \sim 0.01$.

7. SUMMARY

1. – A gamma ray that is created below the threshold energy for pair conversion can adiabatically convert to bound positronium (Wunner et al. 1985; Shabad & Usov 1986). We show that such a positronium atom is rapidly dissociated in the presence of an intense flux of thermal X-rays from the magnetar surface, through the resonant absorption of an X-ray by one of the two charges. Positronium is also photodissociated by infrared radiation if the surface luminosity at ~ 0.1 eV exceeds $\sim 10^{29}$ ergs s^{-1} . This minimum luminosity is only $\sim 10^{-2} - 10^{-3}$ of the observed infrared output of the AXPs, but some $\sim 10^6$ times the flux expected from the Rayleigh-Jeans tail of the X-ray blackbody.

2. – We have calculated the cross section for the reaction $\gamma + \gamma \rightarrow e^+ + e^-$ in the presence of an ultrastrong magnetic field, using electron wavefunctions that are eigenstates of the electron spin. We find a resonance in the cross section when the gamma ray is, by itself, just below the threshold energy for pair creation. Away from this resonance, the value of the cross section differs slightly from previous results.

3. – We have considered the generation of e^\pm pairs when the magnetic field lines are strongly turbulent, and have found a self-consistent state with a very high pair density and a low mean energy per particle. In this situation, a high-frequency spectrum of Alfvén waves is created via a turbulent cascade. The current density diverges in this cascade. There is a critical wave frequency above which the plasma is not able to support the current, and the energy of the waves is transferred to the longitudinal motion of the charges. When the pair density is high, particles are heated close to the star, where resonant scattering is effective. There is a critical spin period of $\sim 5 - 7$ seconds, below which the pair creation rate in this inner zone is high enough to compensate the loss of pairs across the light cylinder and into the pulsar wind. This result does not depend on the details of the particle distribution function within the circuit.

4. – The timescale for the ohmic evolution of the twist in the outer magnetosphere is relatively short (~ 0.1 day). The fast variability that is observed in the brightness of the radio magnetars therefore has a plausible explanation in terms of current-driven instabilities on the closed magnetic field lines.

5. – We have described in some detail a conjecture that the outer magnetosphere can remain strongly twisted only when the pair density is very high on the open magnetic field lines. In this possible metastable state, the loss of magnetic helicity across the magnetospheric boundary is just high enough to sustain large fluctuations in the twist, and high rates of pair creation. Part of the motivation comes from the consideration of the growth of current-driven instabilities in the outer magnetosphere, which are strongly enhanced if the sign of the current on the open field lines matches that flowing into the polar regions of the rotationally-driven wind.

6. – The cumulative torque that can be exerted on the spin of a magnetar in the active magnetospheric phase has been considered, and it has been shown that it can exceed the cumulative magnetic dipole torque. For this reason, the observed clustering of magnetar spins may be connected to a loss of stability of a twisted magnetosphere at a characteristic spin period of several seconds

As is discussed in further detail in Thompson (2008), the dynamic model of the outer magnetosphere investigated here has a promising application to the radio magnetars, in particular to their hard spectra, broad pulses, and relatively high luminosities (in comparison with the spindown luminosity). The consistency of this pair-rich circuit solution does not, by itself, imply a radio death line for magnetars – a weaker pair discharge appears possible at significantly longer spin periods (e.g. Medin & Lai 2007). However, radio emission from the inner magnetosphere would be much harder to detect, due to the effects of beaming.

This work was supported by the NSERC of Canada. I am indebted to Andrei Beloborodov for explaining some of the literature

on positronium creation to me. His suggestion that a hybrid gamma-ray/electron-positron pair might be able to photodissociate led to the calculation in §A.2. I also thank Cornell University for its hospitality when part of this work was completed.

REFERENCES

- Adler, S. L. 1971, *Annals of Physics*, 67, 599
 Baring, M. G., & Harding, A. K. 1998, *ApJ*, 507, L55
 Baring, M. G., & Harding, A. K. 2001, *ApJ*, 547, 929
 Baring, M. G., & Harding, A. K. 2007, *Ap&SS*, 308, 109
 Beloborodov, A. M., & Thompson, C. 2007, *ApJ*, 657, 967
 Berestetskii, V.B., Lifshitz, E.M., & Pitaevskii, L.P. 1982, Oxford: Pergamon Press
 Camilo, F., Ransom, S. M., Halpern, J. P., Reynolds, J., Helfand, D. J., Zimmerman, N., & Sarkissian, J. 2006, *Nature*, 442, 892
 Camilo, F., et al. 2007a, *ApJ*, 663, 497
 Camilo, F., Ransom, S. M., Halpern, J. P., & Reynolds, J. 2007b, *ApJ*, 666, L93
 Camilo, F., Reynolds, J., Johnston, S., Halpern, J. P., & Ransom, S. M. 2008, *ArXiv e-prints*, 802, arXiv:0802.0494
 Chang, H.-K. 1995, *A&A*, 301, 456
 Cheng, K. S., Ho, C., & Ruderman, M. 1986, *ApJ*, 300, 500
 Cheng, K. S., & Zhang, L. 2001, *ApJ*, 562, 918
 Daugherty, J. K., & Ventura, J. 1978, *Phys. Rev. D*, 18, 1053
 Daugherty, J. K., & Harding, A. K. 1989, *ApJ*, 336, 861
 Dermer, C. D. 1990, *ApJ*, 360, 197
 Durant, M., & van Kerkwijk, M. H. 2006a, *ApJ*, 650, 1070
 Durant, M., & van Kerkwijk, M. H. 2006b, *ApJ*, 650, 1082
 Erber, T. 1966, *Reviews of Modern Physics*, 38, 626
 Fernández, R., & Thompson, C. 2007, *ApJ*, 660, 615
 Goldreich, P., & Julian, W. H. 1969, *ApJ*, 157, 869
 Goldreich, P., & Sridhar, S. 1995, *ApJ*, 438, 763
 Gonthier, P. L., Harding, A. K., Baring, M. G., Costello, R. M., & Mercer, C. L. 2000, *ApJ*, 540, 907
 Gotthelf, E. V., & Halpern, J. P. 2005, *ApJ*, 632, 1075
 Halpern, J. P., & Gotthelf, E. V. 2005, *ApJ*, 618, 874
 Herold, H. 1979, *Phys. Rev. D*, 19, 2868
 Herold, H., Ruder, H., & Wunner, G. 1985, *Physical Review Letters*, 54, 1452
 Hirschman, J. A., & Arons, J. 2001a, *ApJ*, 554, 624
 Hirschman, J. A., & Arons, J. 2001b, *ApJ*, 560, 871
 Ibrahim, A. I., et al. 2001, *ApJ*, 558, 237
 Johnson, M. H., & Lippmann, B. A. 1949, *Physical Review*, 76, 828
 Kardashev, N. S., Mitrofanov, N. S., & Novikov, I. D. 1984, *AZh*, 61, 1113
 Kaspi, V. M., Gavriil, F. P., Chakrabarty, D., Lackey, J. R., & Munro, M. P. 2001, *ApJ*, 558, 253
 Kozlenkov, A. A., & Mitrofanov, I. G. 1986, *Zhurnal Eksperimental noi i Teoreticheskoi Fiziki*, 91, 1978
 Kuiper, L., Hermsen, W., & Mendez, M. 2004, *ApJ*, 613, 1173
 Kuiper, L., Hermsen, W., den Hartog, P. R., & Collmar, W. 2006, *ApJ*, 645, 556
 Lieb, E. H., Solovej, J. P., & Yngvason, J. 1992, *Physical Review Letters*, 69, 749
 Lyutikov, M., & Thompson, C. 2005, *ApJ*, 634, 1223
 Lyutikov, M., & Gavriil, F. P. 2006, *MNRAS*, 368, 690
 Medin, Z., & Lai, D. 2007, *MNRAS*, 1065
 Melrose, D. B., & Parle, A. J. 1983a, *Australian Journal of Physics*, 36, 755
 Melrose, D. B., & Parle, A. J. 1983b, *Australian Journal of Physics*, 36, 799
 Mereghetti, S., Götz, D., Mirabel, I. F., & Hurlley, K. 2005, *A&A*, 433, L9
 Padden, W. E. P. 1994, *Journal of Physics B Atomic Molecular Physics*, 27, 5419
 Potekhin, A. Y., & Pavlov, G. G. 1997, *ApJ*, 483, 414
 Psaltis, D., & Miller, M. C. 2002, *ApJ*, 578, 325
 Rea, N., et al. 2006, preprint (astro-ph/0610802)
 Sasaki, M., Plucinsky, P. P., Gaetz, T. J., Smith, R. K., Edgar, R. J., & Slane, P. O. 2004, *ApJ*, 617, 322
 Shabad, A. E., & Usov, V. V. 1982, *Nature*, 295, 215
 Shabad, A. E., & Usov, V. V. 1984, *Ap&SS*, 102, 327
 Shabad, A. E., & Usov, V. V. 1985, *Ap&SS*, 117, 309
 Shabad, A. E., & Usov, V. V. 1986, *Ap&SS*, 128, 377
 Silantev, N. A., & Iakovlev, D. G. 1980, *Ap&SS*, 71, 45
 Sokolov, A. A., & Ternov, I. M. 1968, *Synchrotron Radiation* (Oxford: Pergamon)
 Spitkovsky, A. 2006, *ApJ*, 648, L51
 Stix, T. H. 1976, *Physical Review Letters*, 36, 521
 Sturmer, S. J. 1995, *ApJ*, 446, 292
 Sturrock, P. A. 1971, *ApJ*, 164, 529
 Thompson, C., *ApJ*, submitted (arXiv:0802.2572)
 Thompson, C., & Blaes, O. 1998, *Phys. Rev. D*, 57, 3219
 Thompson, C., Duncan, R. C., Woods, P. M., Kouveliotou, C., Finger, M. H., & van Paradijs, J. 2000, *ApJ*, 543, 340
 Thompson, C., Lyutikov, M., & Kulkarni, S. R. 2002, *ApJ*, 574, 332
 Thompson, C., & Beloborodov, A. M. 2005, *ApJ*, 635, 565
 Usov, V. V. 2002, *ApJ*, 572, L87
 Usov, V. V., & Melrose, D. B. 1996, *ApJ*, 464, 306
 Wang, Z., Kaspi, V. M., & Higdon, S. J. U. 2007, *ApJ*, 665, 1292
 Wesson, J. 2004, *Tokamaks* (New York: Oxford)
 Woltjer, L. 1958, *ApJ*, 128, 384
 Woods, P. M., Kouveliotou, C., Göğüş, E., Finger, M. H., Swank, J., Markwardt, C. B., Hurlley, K., & van der Klis, M. 2002, *ApJ*, 576, 381
 Woods, P. M., & Thompson, C. 2006, in *Compact Stellar X-ray Sources*, eds. W. H. G. Lewin and M. van der Klis (Cambridge: Cambridge University Press) 547
 Wunner, G., & Herold, H. 1979, *Ap&SS*, 63, 503
 Zhang, B., & Qiao, G. J. 1998, *A&A*, 338, 62

APPENDIX

CALCULATION OF CROSS SECTION FOR $\gamma + \gamma \rightarrow E^+ + E^-$

We summarize our calculation of the creation of an electron-positron pair in an ultrastrong magnetic field, via the collision of two photons. The basic strategy is to calculate the tree level matrix elements illustrated in Fig. 4, using magnetized wavefunctions for the outgoing electron and positron and the virtual electron. In this section, we use naturalized units in which $\hbar = c = 1$.

We focus on two special cases:

1. – The two photons collide head on, each with a center of mass energy $\omega_1 = \omega_2 > m_e$. Their momenta are aligned with the background magnetic field \mathbf{B} . This choice of ingoing momenta corresponds approximately to the case where an energetic gamma-ray is created by resonant scattering of a thermal X-ray by a relativistic charge, in a magnetic field $B < 4B_Q$. Then the gamma ray is below threshold for single-photon pair creation near the point of creation, $\omega_1 \sin \theta_{kB,1} < 2m_e$, but it can create a pair by colliding with a thermal X-ray. In the frame where the net momentum parallel to \mathbf{B} vanishes, $k_{1,z} + k_{2,z} = 0$, the target X-ray propagates nearly parallel to \mathbf{B} , and the gamma ray propagates at a modest angle to the magnetic field.

2. – One of the photons is close to the threshold for single-photon pair creation,

$$\omega_1 \sin \theta_{kB,1} = 2m_e - \Delta E. \quad (\text{A1})$$

We take this photon to propagate perpendicular to \mathbf{B} , $\theta_{kB,1} = \pi/2$, and the target photon parallel to \mathbf{B} (Fig. 1). The second photon need not have a very large energy to permit the creation of an electron and positron.

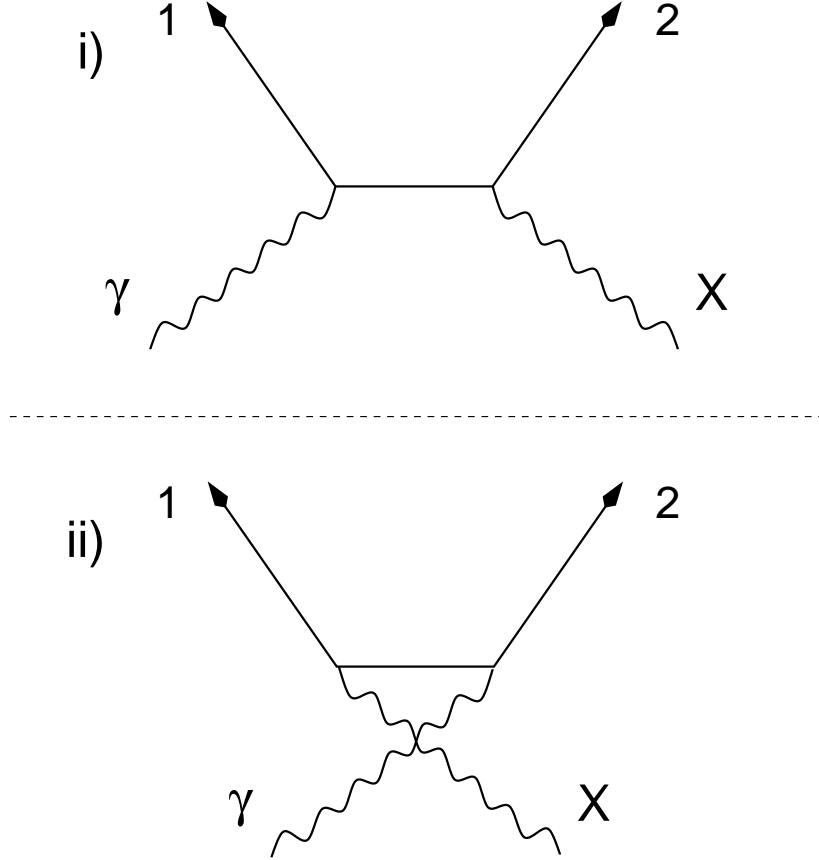


FIG. 4.— Diagrams contributing to the calculation of the cross section for $\gamma + \gamma \rightarrow e^+ + e^-$. In case 1 (head on collision between X-ray and gamma-ray), the outgoing charges 1 and 2 are both in their lowest Landau state $n = 0$. In case 2 (gamma ray near threshold for pair single-photon pair creation), the charge that shares a vertex with the gamma-ray ends up in Landau state $n = 0$, and the charge which shares a vertex with the X-ray ends up in the state $n = 1$. When the interaction between the two photons is resonant, there is no interference between the two channels.

A calculation of the cross section for $\gamma + \gamma \rightarrow e^+ + e^-$ in an ultra-strong magnetic field was published by Koslenkov & Mitrofanov (1986) using the Johnson & Lippman (1949) electron/positron wave functions. These wave functions are not, however, eigenstates of the electron spin. We therefore use an alternative form derived by Sokolov & Ternov (1968) and Melrose & Parle (1983).

The solution to the Dirac equation

$$\left[\gamma^\mu \left(i \frac{\partial}{\partial x^\mu} - e A_\mu \right) - m \right] \psi = 0 \quad (\text{A2})$$

is labeled by the component of the spin parallel to the magnetic field, $\sigma \cdot \hat{\mathbf{B}} = \frac{1}{2} \sigma = \pm \frac{1}{2}$, the longitudinal momentum $P = \mathbf{P} \cdot \hat{\mathbf{B}}$, and the Landau level n :

$$\left[\psi_-^{(\sigma)}(\mathbf{x}, t) \right]_{P, n, a} = e^{iP \cdot x} u_{n, a}^{(\sigma)}(\mathbf{x}_\perp), \quad (\text{A3})$$

for the electron (positive-energy) states, and

$$\left[\psi_+^{(\sigma)}(\mathbf{x}, t) \right]_{P, n, a} = e^{-iP \cdot x} v_{n, a}^{(\sigma)}(\mathbf{x}_\perp) \quad (\text{A4})$$

for the positron (negative-energy) states. The dispersion relation is given by

$$E^2 = P^2 + E_{0n}^2 = P^2 + m_e^2 + 2n|e|B, \quad (\text{A5})$$

where P denotes the component of the momentum parallel to \mathbf{B} . The wave function is localized about one of the two coordinates transverse to the magnetic field (the x -coordinate),

$$\mathbf{x}_\perp = a\hat{x}. \quad (\text{A6})$$

The corresponding transverse momentum is

$$\begin{aligned} \mathbf{P}_\perp &= e\mathbf{x}_\perp \times \mathbf{B} \\ &= -aeB\hat{y} \equiv -\frac{a}{\lambda_B^2}\hat{y}. \end{aligned} \quad (\text{A7})$$

In a frame where $P = 0$, the positive-energy wave functions are

$$u_{n,a}^{(-)}(\mathbf{x}_\perp) = \frac{1}{L(2E_{0n})^{1/2}} \begin{bmatrix} 0 \\ (E_{0n} + m_e)^{1/2} \phi_n(x-a) \\ -i(E_{0n} - m_e)^{1/2} \phi_{n-1}(x-a) \\ 0 \end{bmatrix} \quad (n \geq 0) \quad (\text{A8})$$

and

$$u_{n,a}^{(+)}(\mathbf{x}_\perp) = \frac{1}{L(2E_{0n})^{1/2}} \begin{bmatrix} (E_{0n} + m_e)^{1/2} \phi_{n-1}(x-a) \\ 0 \\ 0 \\ i(E_{0n} - m_e)^{1/2} \phi_n(x-a) \end{bmatrix} \quad (n \geq 1), \quad (\text{A9})$$

where L^3 is the normalization volume. The x -dependence of the wave function is

$$\phi_n(x-a) = \frac{1}{(2^n n!)^{1/2}} \left(\frac{eB}{\pi} \right)^{1/4} \exp \left[-\frac{1}{2} \left(\frac{x-a}{\lambda_B} \right)^2 \right] H_n \left(\frac{x-a}{\lambda_B} \right), \quad (\text{A10})$$

where H_n is the Hermite polynomial. In a frame boosted to a momentum P parallel to \mathbf{B} , the wave functions become

$$u_{n,a}^{(-)}(\mathbf{x}_\perp) = \frac{1}{2L[EE_{0n}(E+E_{0n})]^{1/2}} \begin{bmatrix} -iP(E_{0n} - m_e)^{1/2} \phi_{n-1} \\ (E + E_{0n})(E_{0n} + m_e)^{1/2} \phi_n \\ -i(E + E_{0n})(E_{0n} - m_e)^{1/2} \phi_{n-1} \\ -P(E_{0n} + m_e)^{1/2} \phi_n \end{bmatrix}, \quad (\text{A11})$$

$$u_{n,a}^{(+)}(\mathbf{x}_\perp) = \frac{1}{2L[EE_{0n}(E+E_{0n})]^{1/2}} \begin{bmatrix} (E + E_{0n})(E_{0n} + m_e)^{1/2} \phi_{n-1} \\ -iP(E_{0n} - m_e)^{1/2} \phi_n \\ P(E_{0n} + m_e)^{1/2} \phi_{n-1} \\ i(E + E_{0n})(E_{0n} - m_e)^{1/2} \phi_n \end{bmatrix}. \quad (\text{A12})$$

The positron wave functions are given by

$$v_{n,a}^{(-)}(\mathbf{x}_\perp) = \frac{1}{2L[EE_{0n}(E+E_{0n})]^{1/2}} \begin{bmatrix} i(E + E_{0n})(E_{0n} - m_e)^{1/2} \phi_{n-1} \\ -P(E_{0n} + m_e)^{1/2} \phi_n \\ iP(E_{0n} - m_e)^{1/2} \phi_{n-1} \\ (E + E_{0n})(E_{0n} + m_e)^{1/2} \phi_n \end{bmatrix}, \quad (\text{A13})$$

$$v_{n,a}^{(+)}(\mathbf{x}_\perp) = \frac{1}{2L[EE_{0n}(E+E_{0n})]^{1/2}} \begin{bmatrix} P(E_{0n} + m_e)^{1/2} \phi_{n-1} \\ -i(E + E_{0n})(E_{0n} - m_e)^{1/2} \phi_n \\ (E + E_{0n})(E_{0n} + m_e)^{1/2} \phi_{n-1} \\ iP(E_{0n} - m_e)^{1/2} \phi_n \end{bmatrix}. \quad (\text{A14})$$

In these expressions, E_{0n} is the energy at $P = 0$, and $E = E(P)$ (eq. [A5]).

The wavefunctions of the two photons (four-momenta $k_i = (\omega_i, \mathbf{k}_i)$, polarization vectors ε_i^μ , $i = 1, 2$) are normalized in the usual way,

$$A_i^\mu(x) = \frac{e^{ik_i \cdot x}}{(2\omega_i)^{1/2} L^{3/2}} \varepsilon_i^\mu. \quad (\text{A15})$$

Case 1: Head on Collision, Center-of-Momentum Frame

We consider the photon collision not too far above the threshold for pair creation, in a range of energies where the outgoing electron and positron must be confined to their lowest Landau states, $n_- = n_+ = 0$. We work in the center-of-momentum frame where

$$\omega_1 = k_{1,z} = \omega; \quad \omega_2 = -k_{1,z} = \omega. \quad (\text{A16})$$

The energies and momenta of the outgoing electron and positron are then

$$E_- = E_+ = \omega \quad P_- = -P_+ = \sqrt{\omega^2 - m_e^2}. \quad (\text{A17})$$

We calculate the matrix elements

$$S_{fi} = S_{fi}[1] + S_{fi}[2]; \quad (\text{A18})$$

$$\begin{aligned}
S_{fi}[1] &= ie^2 \int d^4x \int d^4x' [\bar{\psi}_-^{(-1)}(x')]_{n=0} \gamma_\mu A_2^\mu(x') G_F(x'-x) \gamma_\nu A_1^\nu(x) [\psi_+^{(-1)}(x)]_{n_+=0}; \\
S_{fi}[2] &= ie^2 \int d^4x \int d^4x' [\bar{\psi}_-^{(-1)}(x')]_{n=0} \gamma_\mu A_1^\mu(x') G_F(x'-x) \gamma_\nu A_2^\nu(x) [\psi_+^{(-1)}(x)]_{n_+=0},
\end{aligned} \tag{A19}$$

using the real-space representation of the electron propagator

$$\begin{aligned}
G_F(x'-x) &= L^2 \int \frac{da_I}{2\pi\lambda_B^2} \int \frac{dP_I}{2\pi} \sum_{n_I=0}^{\infty} \left[-i\theta(t'-t) \sum_{\sigma_I} u_{n_I}^{(\sigma_I)}(\mathbf{x}') \bar{u}_{n_I}^{(\sigma_I)}(\mathbf{x}) e^{-iE_I(t'-t)} e^{i\mathbf{p}\cdot(\mathbf{x}'-\mathbf{x})} \right. \\
&\quad \left. + i\theta(t-t') \sum_{\sigma_I} v_{n_I}^{(\sigma_I)}(\mathbf{x}') \bar{v}_{n_I}^{(\sigma_I)}(\mathbf{x}) e^{iE_I(t'-t)} e^{-i\mathbf{p}\cdot(\mathbf{x}'-\mathbf{x})} \right].
\end{aligned} \tag{A20}$$

Here $\bar{\psi} = \psi^\dagger \gamma_0 = (\psi^*)^T \gamma_0$, where $*$ denotes complex conjugation and T the transpose. Performing the integrals over t, t' yields a factor $2\pi\delta(E_+ + E_- - \omega_1 - \omega_2)(E_- - \omega_2 \mp E_I)^{-1}$ for each of the two terms in G_F , and we have

$$\begin{aligned}
S_{fi}[1] &= -\frac{ie^2}{2\omega} \frac{1}{L^3} \left(\frac{L}{2\pi} \right)^2 2\pi\delta(E_+ + E_- - 2\omega) \\
&\quad \times \int dP_I \int \frac{da_I}{\lambda_B^2} \sum_{\sigma_I} \int \left(\frac{I_1^{(\sigma_I)} I_2^{(\sigma_I)}}{E_- - \omega - E_I} + \frac{I_3^{(\sigma_I)} I_4^{(\sigma_I)}}{E_- - \omega + E_I} \right),
\end{aligned} \tag{A21}$$

where

$$\begin{aligned}
I_1^{(\sigma_I)} &= \int d^3x' [\bar{u}_{0,a_-}^{(-1)}(\mathbf{x}'_\perp) \gamma_\mu u_{1,a_I}^{(\sigma_I)}(\mathbf{x}'_\perp)] \varepsilon_2^\mu e^{i(\mathbf{k}_2 - \mathbf{p}_- + \mathbf{p}_I) \cdot \mathbf{x}'}; \\
I_2^{(\sigma_I)} &= \int d^3x [\bar{u}_{1,a_I}^{(\sigma_I)}(\mathbf{x}_\perp) \gamma_\nu v_{0,a_+}^{(-1)}(\mathbf{x}_\perp)] \varepsilon_1^\nu e^{i(\mathbf{k}_1 - \mathbf{p}_+ - \mathbf{p}_I) \cdot \mathbf{x}}; \\
I_3^{(\sigma_I)} &= \int d^3x' [\bar{u}_{0,a_-}^{(-1)}(\mathbf{x}'_\perp) \gamma_\mu v_{1,a_I}^{(\sigma_I)}(\mathbf{x}'_\perp)] \varepsilon_2^\mu e^{i(\mathbf{k}_2 - \mathbf{p}_+ - \mathbf{p}_I) \cdot \mathbf{x}'}; \\
I_4^{(\sigma_I)} &= \int d^3x [\bar{v}_{1,a_I}^{(\sigma_I)}(\mathbf{x}_\perp) \gamma_\nu v_{0,a_+}^{(-1)}(\mathbf{x}_\perp)] \varepsilon_1^\nu e^{i(\mathbf{k}_1 - \mathbf{p}_+ + \mathbf{p}_I) \cdot \mathbf{x}}.
\end{aligned} \tag{A22}$$

These integrals involve a matrix

$$\gamma_0 \gamma_\nu \varepsilon_i^\mu = \begin{pmatrix} 1 & 0 \\ 0 & -1 \end{pmatrix} \varepsilon_i^t + \begin{pmatrix} 0 & \sigma_x \\ \sigma_x & 0 \end{pmatrix} \varepsilon_i^x + \begin{pmatrix} 0 & \sigma_y \\ \sigma_y & 0 \end{pmatrix} \varepsilon_i^y + \begin{pmatrix} 0 & \sigma_z \\ \sigma_z & 0 \end{pmatrix} \varepsilon_i^z, \tag{A23}$$

where σ_i are the 2×2 Pauli matrices. Expanding, one finds

$$\gamma_0 \gamma_\nu \varepsilon_i^\mu = \begin{pmatrix} 0 & 0 & \varepsilon_i^z & \varepsilon_i^- \\ 0 & 0 & \varepsilon_i^+ & -\varepsilon_i^- \\ \varepsilon_i^z & \varepsilon_i^- & 0 & 0 \\ \varepsilon_i^+ & -\varepsilon_i^- & 0 & 0 \end{pmatrix}, \tag{A24}$$

where $\varepsilon_i^\pm = \varepsilon_i^x \pm i\varepsilon_i^y$.

It will be noted that only the Landau level $n_I = 1$ in the propagator contributes to the matrix element. That is because

$$\bar{u}_{0,a_1}^{(-1)} \gamma_\mu u_{0,a_2}^{(-1)} \varepsilon_i^\mu \propto \varepsilon_i^z \tag{A25}$$

vanishes when the two photons are incident parallel to \mathbf{B} , and because integrals of the form

$$\int d^2x_\perp \phi_0(x-a_1) \phi_m(x-a_2) e^{i(\mathbf{k}_i - \mathbf{p}_+ + \mathbf{p}_I)_\perp \cdot \mathbf{x}_\perp} \propto |\mathbf{k}_{i,\perp}|^m \tag{A26}$$

also vanish when $m \geq 1$. We are therefore left with evaluating integrals of the form

$$\int d^3x \phi_0(x-a_1) \phi_0(x-a_2) e^{i(\mathbf{k}_i - \mathbf{p}_1 + \mathbf{p}_2) \cdot \mathbf{x}} = \left(\frac{2\pi}{L} \right)^2 \delta \left(\frac{a_1 - a_2}{\lambda_B^2} \right) \delta(k_{i,z} - P_1 + P_2), \tag{A27}$$

where the result assumes $\mathbf{k}_{i,\perp} = 0$. For example, the integrals I_1, I_2 take the form

$$I_1^{(\sigma_I)} = \frac{F_1^{(\sigma_I)} \varepsilon_2^+}{4[E_- E_I m_e E_{0n} (E_- + m_e) (E_I + E_{0n})]^{1/2}} \left(\frac{2\pi}{L} \right)^2 \delta \left(\frac{a_- - a_I}{\lambda_B^2} \right) \delta(k_{2,z} - P_- + P_I), \tag{A28}$$

$$I_2^{(\sigma_I)} = \frac{F_2^{(\sigma_I)} \varepsilon_1^-}{4[E_+ E_I m_e E_{0n} (E_+ + m_e)(E_I + E_{0n})]^{1/2}} \left(\frac{2\pi}{L} \right)^2 \delta \left(\frac{a_I - a_+}{\lambda_B^2} \right) \delta(k_{1,z} - P_+ - P_I), \quad (\text{A29})$$

where

$$E_{0n} \equiv (m_e^2 + 2eB)^{1/2}; \quad E_I \equiv [(\omega + P_-)^2 + m_e^2 + 2eB]^{1/2} \quad (\text{A30})$$

and

$$\begin{aligned} F_1^{(-1)} &= i \left[P_- P_I - (E_- + m_e)(E_I + E_{0n}) \right] (2m_e)^{1/2} (E_{0n} - m_e)^{1/2}; \\ F_1^{(+1)} &= \left[(E_- + m_e) P_I - (E_I + E_{0n}) P_- \right] (2m_e)^{1/2} (E_{0n} + m_e)^{1/2}; \\ F_2^{(-1)} &= i \left[(E_+ + m_e) P_I - (E_I + E_{0n}) P_+ \right] (2m_e)^{1/2} (E_{0n} - m_e)^{1/2}; \\ F_2^{(+1)} &= \left[P_+ P_I - (E_+ + m_e)(E_I + E_{0n}) \right] (2m_e)^{1/2} (E_{0n} + m_e)^{1/2}. \end{aligned} \quad (\text{A31})$$

Summing gives

$$\begin{aligned} I_1^{(-1)} I_2^{(-1)} + I_1^{(+1)} I_2^{(+1)} &= \varepsilon_1^- \varepsilon_2^+ \frac{m_e (P_I - P_{\pm})}{2E_{\pm} E_I} \left(\frac{2\pi}{L} \right)^4 \delta \left(\frac{a_- - a_I}{\lambda_B^2} \right) \delta \left(\frac{a_+ - a_I}{\lambda_B^2} \right) \\ &\quad \times \delta(\omega + P_- - P_I) \delta(\omega - P_+ - P_I). \end{aligned} \quad (\text{A32})$$

and

$$\begin{aligned} I_3^{(-1)} I_4^{(-1)} + I_3^{(+1)} I_4^{(+1)} &= \varepsilon_1^- \varepsilon_2^+ \frac{m_e (P_I + P_{\pm})}{2E_{\pm} E_I} \left(\frac{2\pi}{L} \right)^4 \delta \left(\frac{a_- + a_I}{\lambda_B^2} \right) \delta \left(\frac{a_+ + a_I}{\lambda_B^2} \right) \\ &\quad \times \delta(\omega + P_- + P_I) \delta(\omega - P_+ + P_I). \end{aligned} \quad (\text{A33})$$

We have used the notation $P_{\pm} = P_- = -P_+$ and $E_{\pm} = E_+ = E_-$, and substituted $k_{1,z} = -k_{2,z} = \omega$.

The first term in the matrix element is obtained by substituting eqs. (A32) and (A33) into eq. (A21),

$$S_{fi}[1] = -\frac{ie^2}{2L^5} \frac{m_e \varepsilon_1^- \varepsilon_2^+}{\omega [(\omega + P_-)^2 + m_e^2 + 2eB]} (2\pi)^3 \delta(E_- + E_+ - 2\omega) \delta(P_+ + P_-) \delta \left(\frac{a_- - a_+}{\lambda_B^2} \right). \quad (\text{A34})$$

The second contribution to the matrix element is obtained by exchanging the two photons, which corresponds to taking $P_I \rightarrow P_- - \omega$ in the denominator,

$$S_{fi}[2] = \frac{ie^2}{2L^5} \frac{m_e \varepsilon_1^+ \varepsilon_2^-}{\omega [(\omega - P_-)^2 + m_e^2 + 2eB]} (2\pi)^3 \delta(E_- + E_+ - 2\omega) \delta(P_+ + P_-) \delta \left(\frac{a_- - a_+}{\lambda_B^2} \right). \quad (\text{A35})$$

The total cross section for $\gamma + \gamma \rightarrow e^+ + e^-$, with the electron and positron both in the lowest Landau state, is obtained from

$$(1 - \cos \theta_{12}) \sigma = \frac{L^3}{T} \int L \frac{da_-}{2\pi \lambda_B^2} \int L \frac{da_+}{2\pi \lambda_B^2} \int L \frac{dp_-}{2\pi} \int L \frac{dp_+}{2\pi} \left| S_{fi}[1] + S_{fi}[2] \right|^2. \quad (\text{A36})$$

Here $\cos \theta_{12} = -1$ is the cosine of the collision angle between the two photons, and T is a normalization time. The square of a delta function is handled with the substitution $[(2\pi) \delta(E_- + E_+ - 2\omega)]^2 \rightarrow T (2\pi) \delta(E_- + E_+ - 2\omega)$, $[(2\pi) \delta(P_+ + P_-)]^2 \rightarrow L (2\pi) \delta(P_+ + P_-)$, and so on, yielding

$$\sigma = \frac{e^4}{32\pi\omega^2} \left(\frac{B}{B_Q} \right) \left| \frac{dE_{\pm}}{dP_{\pm}} \right|^{-1} \left| \frac{\varepsilon_2^+ \varepsilon_1^- m_e^2}{(\omega + P_{\pm})^2 + m_e^2 + 2eB} - \frac{\varepsilon_1^+ \varepsilon_2^- m_e^2}{(\omega - P_{\pm})^2 + m_e^2 + 2eB} \right|^2. \quad (\text{A37})$$

Here $dE_{\pm}/dP_{\pm} = V_{\pm}$ is the speed of the outgoing electron and positron. The coefficient in front is readily expressed in terms of the Thomson cross section

$$\sigma_T = \frac{8\pi}{3} \left(\frac{e^2}{4\pi m_e} \right)^2. \quad (\text{A38})$$

Near threshold, the cross section vanishes if the two photons have the same linear polarization,

$$\frac{\sigma}{\sigma_T} = \frac{3B/B_Q}{16(1+B/B_Q)^2} \left(\frac{V_{\pm}}{c} \right)^{-1} (\varepsilon_1^x \varepsilon_2^y - \varepsilon_2^x \varepsilon_1^y)^2 \quad (\omega \rightarrow m_e). \quad (\text{A39})$$

Case 2: Photon 1 Near Threshold for Pair Creation

We now turn to the case where one photon (labeled 1) is just below threshold for pair creation. We choose a frame in which $\omega_1 = 2m_e - \Delta E$, $k_{1,z} = 0$, and $\omega_2 = k_{2,z}$. We focus on the case where there is a near resonance in the matrix element, in the sense that the virtual electron is nearly on mass shell. Simple kinematic considerations show that this corresponds to one outgoing particle in the first Landau state, with the virtual particle in level $n_l = 0$ (§3). The final-state particle in state $n = 1$ is the one that shares a vertex with photon 2 in Fig. 4. The final states with $n_- = 1, n_+ = 0$ and $n_- = 0, n_+ = 1$ are distinguishable, and so we may calculate the cross section for the electron in the excited state, and then multiply by a factor 2 to obtain the total cross section. The excited particle also comes in two spin states $\sigma = \pm 1$, which must be summed over.

The matrix elements to be calculated are therefore

$$S_{fi}^{(\sigma_-)} = ie^2 \int d^4x \int d^4x' [\bar{\psi}_-^{(\sigma_-)}(x')]_{n_- = 1} \gamma_\mu A_2^\mu(x') G_F(x' - x) \gamma_\nu A_1^\nu(x) [\psi_+^{(-1)}(x)]_{n_+ = 0} \quad (\sigma_- = \pm 1), \quad (\text{A40})$$

and the cross section is given by

$$(1 - \cos\theta_{12})\sigma = 2 \frac{L^3}{T} \int L \frac{da_-}{2\pi\lambda_B^2} \int L \frac{da_+}{2\pi\lambda_B^2} \int L \frac{dp_-}{2\pi} \int L \frac{dp_+}{2\pi} \left(|S_{fi}^{(-1)}|^2 + |S_{fi}^{(+1)}|^2 \right), \quad (\text{A41})$$

where in this case $\cos\theta_{12} = 0$. The condition for a near resonance is that $E_l \simeq E_- - \omega_2$, and so we need only include the term in expression (A20) for $G_F(x' - x)$ involving the positive-energy wavefunctions. The matrix elements (A40) become

$$S_{fi}^{(\sigma_-)} = -\frac{ie^2}{2(\omega_1\omega_2)^{1/2}} \frac{1}{L^3} \left(\frac{L}{2\pi} \right)^2 2\pi\delta(E_+ + E_- - \omega_1 - \omega_2) \int \frac{da_l}{\lambda_B^2} \int dp_l \frac{I_1^{(\sigma_-)} I_2}{E_- - \omega_2 - E_l}, \quad (\text{A42})$$

where

$$\begin{aligned} I_1^{(\sigma_-)} &= \int d^3x' [\bar{u}_{1,a_-}^{(\sigma_-)}(\mathbf{x}'_\perp) \gamma_\mu u_{0,a_l}^{(-1)}(\mathbf{x}'_\perp)] \varepsilon_2^\mu e^{i(\mathbf{k}_2 - \mathbf{p}_+ + \mathbf{p}_l) \cdot \mathbf{x}'}; \\ I_2 &= \int d^3x [\bar{u}_{0,a_l}^{(-1)}(\mathbf{x}_\perp) \gamma_\nu v_{0,a_+}^{(-1)}(\mathbf{x}_\perp)] \varepsilon_1^\nu e^{i(\mathbf{k}_1 - \mathbf{p}_+ + \mathbf{p}_l) \cdot \mathbf{x}}. \end{aligned} \quad (\text{A43})$$

Near threshold for pair creation, one has $E_+ = E_l \simeq m_e$, $E_- \simeq m_e + eB/m_e$, and $\omega_2 \simeq eB/m_e$. The above integrals may then be evaluated as

$$I_1^{(\sigma_-)} = \frac{F_1^{(\sigma_-)} \varepsilon_2^-}{2[E_- E_{0n}(E_{0n} + m_e)(E_- + E_{0n})]^{1/2}} \left(\frac{2\pi}{L} \right)^2 \delta\left(\frac{a_- - a_l}{\lambda_B^2}\right) \delta(k_{2,z} - P_- + P_l); \quad (\text{A44})$$

$$I_2 = \varepsilon_1^z \exp\left(-\frac{\lambda_B^2 \omega_1^2}{4}\right) \left(\frac{2\pi}{L} \right)^2 \delta\left(\omega_1 - \frac{a_+ - a_l}{\lambda_B^2}\right) \delta(P_- + P_+), \quad (\text{A45})$$

where

$$F_1^{(-1)} = i(E_- + E_{0n})(2eB)^{1/2}; \quad F_1^{(+1)} = P_-(E_{0n} + m_e), \quad (\text{A46})$$

and we have chosen the momentum of photon 1 to point in the y-direction. The cross section is proportional to

$$\frac{|F_1^{(-1)}|^2 + |F_1^{(+1)}|^2}{4E_- E_{0n}(E_{0n} + m_e)(E_- + E_{0n})} \simeq \frac{E_- - m_e}{2E_-} = \frac{B/B_Q}{2(1 + B/B_Q)}. \quad (\text{A47})$$

Substituting eqs. (A43)-(A45) into (A42), and averaging over the spins of photon 2, one finds

$$\sigma = \frac{e^4}{16\pi(\omega_1 - 2E_+)^2} \exp\left(-\frac{\omega_1^2}{2eB}\right) \left(\frac{B/B_Q}{1 + B/B_Q} \right) \left| \frac{dP_+}{d(E_- + E_+)} \right|_{P_- + P_+ = \omega_2} (\varepsilon_1^z)^2. \quad (\text{A48})$$

As expected, the cross section is non-vanishing only if photon 1 is polarized parallel to \mathbf{B} . The last factor is determined by differentiating

$$E_- + E_+ = (P_-^2 + m_e^2 + 2eB)^{1/2} + (P_+^2 + m_e^2)^{1/2} \quad (\text{A49})$$

with $P_- = \omega_2 - P_+$. Near threshold,

$$\left| \frac{dP_+}{d(E_- + E_+)} \right|_{P_- + P_+ = \omega_2} \simeq \frac{1 + B/B_Q}{B/B_Q}, \quad (\text{A50})$$

and we have

$$\sigma = \frac{e^4}{16\pi(\omega_1 - 2E_+)^2} \exp\left(-\frac{\omega_1^2}{2eB}\right) (\varepsilon_1^z)^2. \quad (\text{A51})$$

The cross section can then be expressed in terms of σ_T (eq. [52]).